ChemPubSoc Europe

DOI: 10.1002/cmdc.201402508

CHEMMEDCHEM Full Papers

Design, Synthesis, and Biological Evaluation of Simplified Side Chain Hybrids of the Potent Actin Binding Polyketides Rhizopodin and Bistramide

Daniel Herkommer,[a] Sandra Dreisigacker,[a] Galina Sergeev,[b] Florenz Sasse,[b] Holger Gohlke,[c] and Dirk Menche*[a]

The natural products rhizopodin and bistramide belong to an elite class of highly potent actin binding agents. They show powerful antiproliferative activities against a range of tumor cell lines, with IC_{50} values in the low-nanomolar range. At the molecular level they disrupt the actin cytoskeleton by binding specifically to a few critical sites of G-actin, resulting in actin filament stabilization. The important biological properties of rhizopodin and bistramide, coupled with their unique and intriguing molecular architectures, render them attractive compounds for further development. However, this is severely hampered by the structural complexity of these metabolites. We initiated an interdisciplinary approach at the interface between molecular modeling, organic synthesis, and chemical biology to support further biological applications. We also wanted to expand structure–activity relationship studies with the goal of accessing simplified analogues with potent biological properties. We report computational analyses of actin–inhibitor interactions involving molecular docking, validated on known actin binding ligands, that show a close match between the crystal and modeled structures. Based on these results, the ligand shape was simplified, and more readily accessible rhizopodin–bistramide mimetics were designed. A flexible and modular strategy was applied for the synthesis of these compounds, enabling diverse access to dramatically simplified rhizopodin–bistramide hybrids. This novel analogue class was analyzed for its antiproliferative and actin binding properties.

Introduction

Along with tubulin, actin is one of the two major components of the eukaryotic cell cytoskeleton. It is involved in separation during cell division and in the organization of the cell shape and polarity. It also plays an essential role in cell locomotion, as well as intracellular transportation.[1] Actin structures are constantly assembled and disassembled in a reversible manner based on a dynamic and sophisticated polymerization/depolymerization equilibrium between monomeric globular actin (G-actin) and double-stranded filamentous actin (F-actin). This process is regulated by a series of actin binding proteins with specific functions.[2] Malfunction in these kinetics has been associated with various diseases,[3] including cancer[4] as well as bacterial and viral (e.g., HIV) infections.[5] This makes the development and molecular-level understanding of potent actin binding agents important research goals, both for potential new therapeutic agents and as biological tools in advancing the understanding and cellular function of actin.[6]

As shown in Figure 1, G-actin is composed of four main subunits: domains 1–4. Assembly of these monomers proceeds in a bidirectional manner, with subunits 1 and 3 being at one

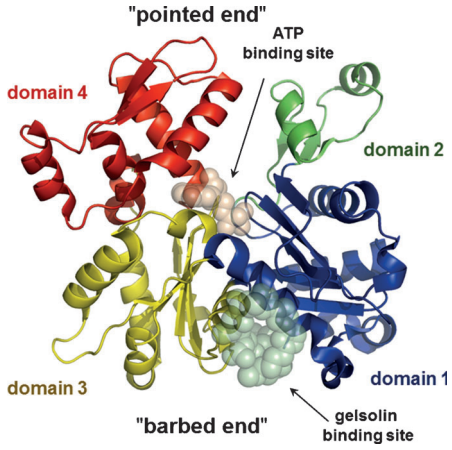

Figure 1. Structure of molecular actin (globular actin; G-actin) with two binding sites for actin polymerization (actin structure taken from the RCSB Protein Data Bank (PDB) ID 1QZ5): a 'pointed end' and a 'barbed end'. The four subdomains are shown in different colors. The ATP binding site (fawn) is located between domains 2 and 4; the binding site for the regulatory protein gelsolin lies between domains 1 and 3. The 'barbed end' inhibitors address the binding site of gelsolin (exemplarily shown for kabiramide C (moss green; PDB ID: 1QZ5)).

[a] D. Herkommer, Dr. S. Dreisigacker, Prof. Dr. D. Menche
Kekulé-Institut für Organische Chemie und Biochemie
Universität Bonn, Gerhard-Domagk-Str. 1, 53121 Bonn (Germany)
E-mail: dirk.menche@uni-bonn.de

[b] Dr. G. Sergeev, Dr. F. Sasse
Chemische Biologie
Helmholtz-Zentrum für Infektionsforschung GmbH
Inhoffenstr. 7, 38124 Braunschweig (Germany)

[c] Prof. Dr. H. Gohlke
Institut für Pharmazeutische und Medizinische Chemie
Heinrich-Heine-Universität Düsseldorf
Universitätsstr. 1, 40225 Düsseldorf (Germany)

Supporting information for this article is available on the WWW under http://dx.doi.org/10.1002/cmdc.201402508.

end ('barbed end') and subunits 2 and 4 at the other side ('pointed end') of the elongating chain.[7] This process is controlled by regulatory proteins, such as gelsolin, which binds between domains 1 and 3, and by hydrolysis of adenosine triphosphate (ATP), which is essential for this process and takes place in a cleft between subunits 2 and 4.

Nature has provided an important source of structurally complex and novel actin binding molecules with filament-stabilizing agents that address the gelsolin binding site.[8,9] As shown in Figure 2, these polyketide natural products include the trisoxazoles (i.e., kabiramides **1**),[10] jaspisamides **2**, ulapualides **3** and halichondramides (not shown),[11] the reidispongiolide/sphinxolide family **4**–**6**,[12] the swinholides **7**,[13] aplyronines **8**,[14] bistramides **9**,[15] lobophorolides **10**,[16] and rhizopodin **11**.[17] All these compounds have been isolated from marine sources, except for rhizopodin, which was isolated from myxobacteria by the research groups of Höfle and Reichenbach at the HZI in Braunschweig.[17a] At the molecular level, they act as actin-filament-stabilizing agents.[8] They demonstrate highly potent binding affinities for G-actin at low-nanomolar concentrations. Furthermore, they exhibit impressive antiproliferative activities against a range of human cancer cell lines with IC_{50} values in the low-nanomolar range. The binding events and molecular influence of these inhibitors on dynamic actin assembly are increasingly well understood. Importantly, X-ray analyses of the corresponding inhibitor–actin complexes have been reported,[18,19] which allow a detailed perception of target–inhibitor interactions at the molecular level. This adds to the attractiveness for further structure–activity relationship (SAR) studies and inhibitor design.

However, further promotion of these highly potent agents is severely hampered by the extremely low natural supply of these scarce natural products. Moreover, structural complexities impede large-scale synthetic access to enable further biological evaluation.[20–23] This renders the development of more readily available analogues critical to enhancing further biological evaluations of these highly promising lead structures. Such development will also allow establishment of further SARs[12f,17d,24–27] to enhance the preclinical advancement of these agents.

Herein, we report in silico studies of the noncovalent actin interactions of these complex polyketides, as well as the design, synthesis, and biological evaluation of a structurally simplified novel analogue class, which is based on a hybrid structure of bistramide and rhizopodin.

Results and Discussion

Modeling noncovalent actin–inhibitor interactions

Analysis of the X-ray structures of actin–ligand complexes revealed three possible binding sites in the cleft between subdomains 1 and 3, which are mainly hydrophobic in nature.[18,19] As shown in Figure 3, the first one is represented by the gelsolin binding site and involves residues Y166, G168, Y169, Y143, T148, T149, I345, L346, L349, T351, F352, and M355. The

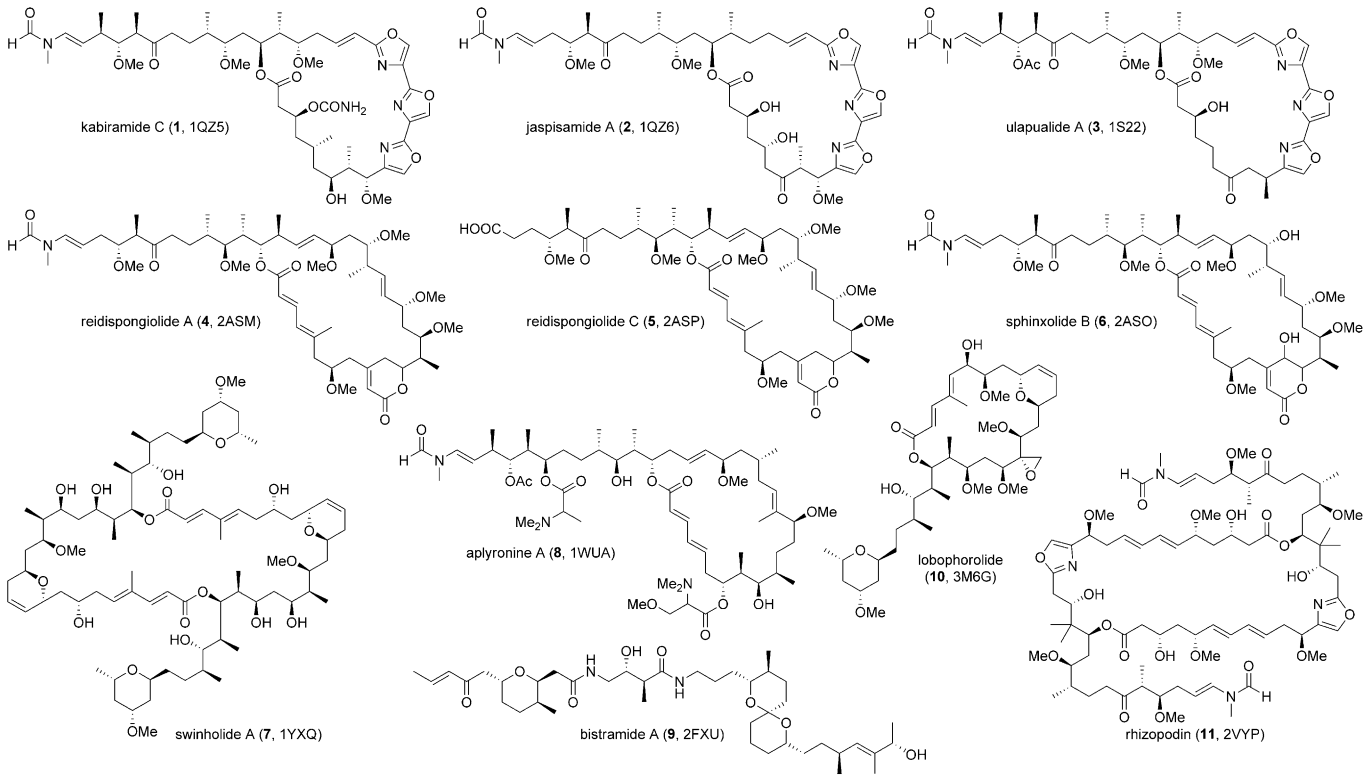

Figure 2. Complex polyketides binding in the cleft between subunits 1 and 3 of G-actin. PDB IDs of the corresponding co-crystals with actin are shown in parentheses. Ac = acetate.

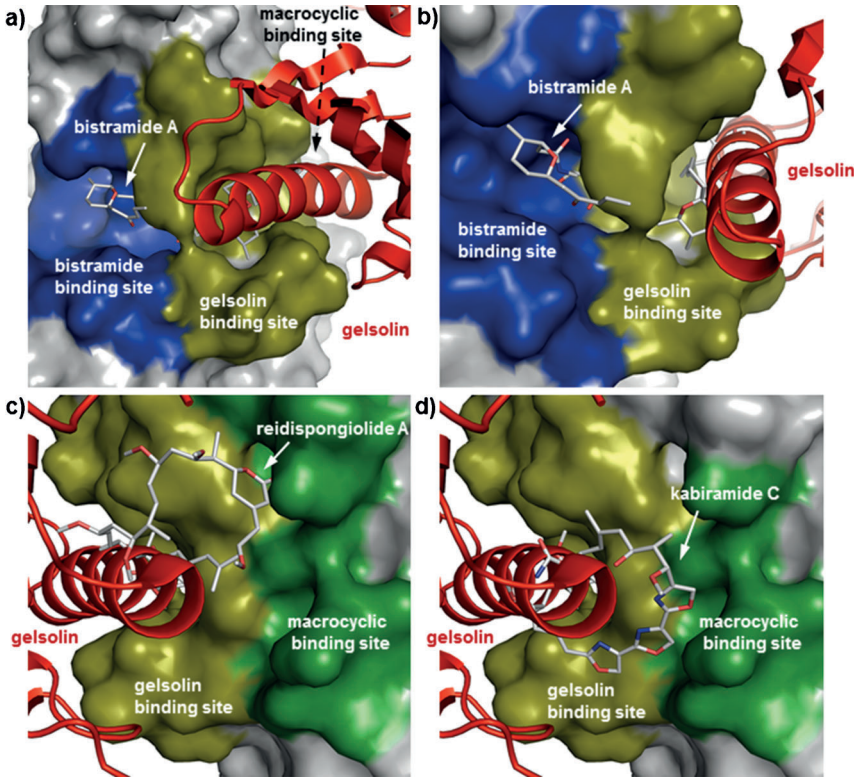

Figure 3. Different perspectives of the possible binding pockets in the cleft between subunits 1 and 3 of G-actin, as derived by X-ray crystallography of actin–inhibitor complexes, as previously reported.[10b,12e,15f] a) Front perspective with bistramide A and gelsolin, b) left-side perspective with bistramide A and gelsolin, c) right side perspective with reidispongiolide A, and d) right side perspective with kabiramide C. The binding pocket for gelsolin is shown in olive, the one for bistramide A in blue, and the one for macrocyclic ligands in green. The binding site of gelsolin partially overlaps with the binding site of macrocyclic ligands as well as with the binding site of bistramide A.[29]

second one partially overlaps with the gelsolin binding site and also includes residues Y133, I136, V139, A170, L171, P172, and F375 inside the hydrophobic pocket at the 'left' of the cleft (Figure 3a,b). This binding site is addressed by the bislactam polyether bistramide A (**9**).[15f] In contrast, all macrocyclic ligands shown in Figure 2, i.e., the trisoxazoles, the reidispongiolide/sphinxolide family, the swinholides, lobophorolides, aplyronines, and rhizopodin, address a third binding domain located at the 'right' of the cleft, also exhibiting partial overlap with the gelsolin binding site (Figure 3c,d).[10b,12e,15f,18,19,28]

Furthermore, these ligands comprise a side chain, which partially overlaps with bistramide A as well as with the gelsolin binding site (exemplarily depicted for rhizopodin in Figure 4). In contrast, the macrocycle of these compounds does not seem to show significant overlap with the bistramide A ligand.

The side chains of the trisoxazoles, reidispongiolide/sphinxolides, aplyronines, and rhizopodin bear remarkable similarities, which has been well documented[11c,d] and explicitly noted.[8,12d,f,17a,18] Importantly, the tail region has been defined as the functional unit of the severing and capping activities of the parent molecule.[8b,12f] In detail, all tail regions have an *N*-methylvinylformamide group at the terminus, two oxygen substituents at C5 and C11, together with two methyl-bearing centers at C6 and C10, and a carbonyl at C7 (Figure 5). Accordingly, the binding modes of these structurally similar side chains in the crystal structures are nearly identical, although the binding modes of the macrocyclic parts of these compounds can be different.

The research groups of Yamada and Marriott have reported that the side chains alone do not retain the activity of the parent natural products.[12f,26,27] Marriott and coworkers also reported the evaluation of a library of tail-region mimetics, demonstrating the significance of an appending hydrophobic protecting group on the terminal hydroxy groups for binding affinity, while the side chain alone is inactive.[12f,26] This is in agreement with an observation reported by Nicolaou and colleagues, who have shown that monomeric rhizopodin retains the actin binding properties of the authentic dimeric natural product.[24]

Thus, the overlapping region of bistramide A and the side chain of the other barbed-end inhibitors around residues G168,

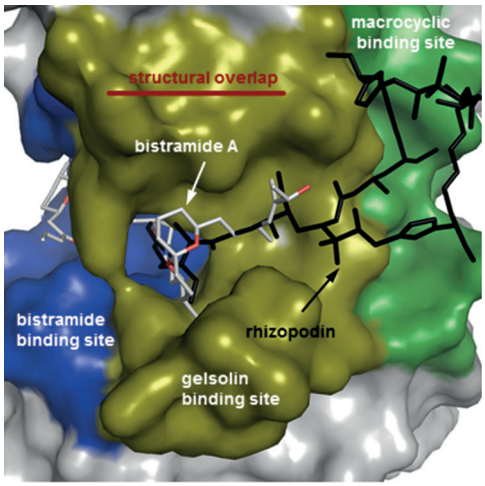

Figure 4. X-ray-derived structural overlap of the binding sites of bistramide A (grey) and the side chains of the macrocyclic 'barbed end' inhibitors, exemplarily shown for rhizopodin (black).

Y169, Y143, T148, I345, L346, L349, T351, F352, and M355, as well as Y133, I136, V139, A170, and F375, appears to be essential for the noncovalent interactions at the actin protein and

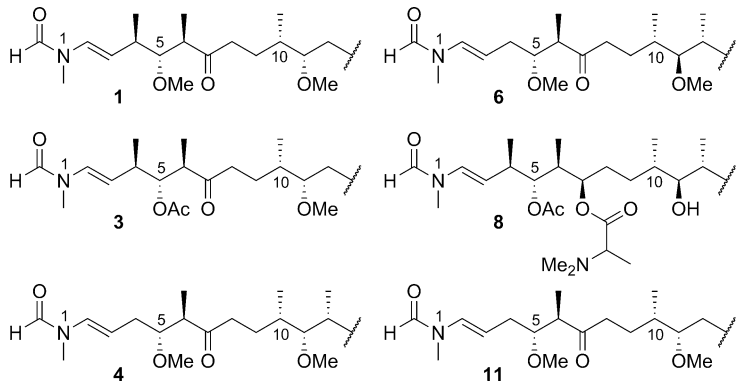

Figure 5. Structural comparison of the vinylformamide side chains of the inhibitors.

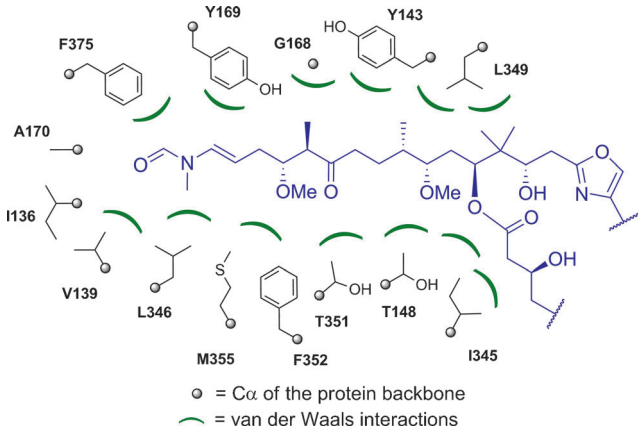

Figure 6. X-ray-derived ligand–receptor interactions of the side chain of 'barbed end' inhibitors with actin. As an example, the side chain and part of the macrocycle of rhizopodin are shown (blue).

therefore presents a promising starting point for the design of effective inhibitors (Figure 6).

We first wanted to evaluate, whether docking by a combination of AutoDock 3.0[30] for binding mode generation, and the DrugScore scoring function[31] for evaluating the binding modes, may be useful for a predictive analysis of this system. Therefore, all inhibitors shown in Figure 2 were re-docked into the actin binding pockets of their corresponding crystal structures. The resulting binding modes were clustered with a root-mean-square deviation (RMSD) value of 1.0 Å (see the Experimental Section and Supporting Information for details). The calculated binding energies of the highest populated clusters and the binding efficiencies with regard to the number of heavy atoms are listed in Table 1.

Analysis of the mean docked energies (red line) revealed the best ligand–receptor interaction for the dimeric ligands, such as swinholide A (PDB ID: 1YXQ) and rhizopodin (2VYP), with respective binding energies of −31.9 and −21.6 kcal mol^{-1}. However, as for the binding efficiencies (blue line) of these differently large ligands, rhizopodin is less potent, with −0.22 kcal mol^{-1}, whereas bistramide A (2FXU) was most effective, showing a binding efficiency of −0.36 kcal mol^{-1} in agreement with the excellent activity data observed for this compound. Rhizopodin and swinholide A are dimeric *C*2-symmetric macrolides; however, their constitutions, particularly of the side chains, are different. The binding energy obtained for lobophorolide A (3M6G) of −11.8 kcal mol^{-1} indicates a poor ligand–receptor interaction for this small ligand. However, its binding efficiency (−0.22 kcal mol^{-1}) is similar to that of rhizopodin (2VYP). This discrepancy most likely arises from the greater number of target–ligand interactions formed by larger ligands than smaller ones, and from the scoring process neglecting changes in configurational entropy upon binding. Therefore, in our study we not only considered the overall binding energy, but also the binding efficiency in relation to the number of heavy atoms. Importantly, only small differences between the calculated binding modes and positions obtained from X-ray crystallographic data were observed, which supports the reliability of this in silico model (see Supporting Information for details).

Table 1. Binding energies of the highest populated clusters obtained from re-docking of the 'barbed end' inhibitors.

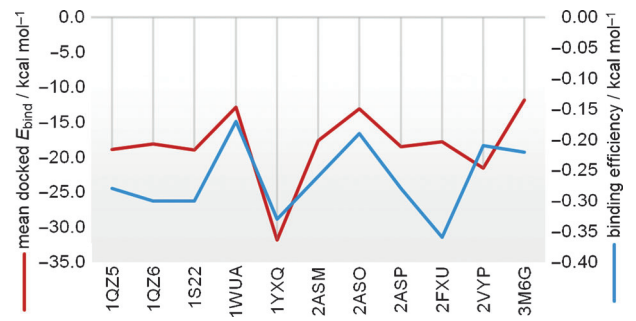

Ligand (PDB ID)	E_{bind} [kcal mol^{-1}][a]	Binding Eff. [kcal mol^{-1}][b]	No. Heavy Atoms[c]	Convergence[d]
1 (1QZ5)	−18.9	−0.28	67	74
2 (1QZ6)	−18.1	−0.30	61	82
3 (1S22)	−19.0	−0.30	63	29
8 (1WUA)	−12.8	−0.17	76	4
7 (1YXQ)	−31.9	−0.33	98	96
4 (2ASM)	−17.6	−0.26	68	81
6 (2ASO)	−13.1	−0.19	68	8
5 (2ASP)	−18.5	−0.28	66	81
9 (2FXU)	−17.8	−0.36	50	3
11 (2VYP)	−21.6	−0.21	104	3
10 (3M6G)	−11.8	−0.22	54	35

[a] Mean docked binding energy of all solutions in the highest populated cluster; the search area included 90 grid points in each dimension,[32] with a grid point distance of 0.375 Å. [b] Binding efficiency: E_{bind} divided by the number of heavy atoms. [c] Number of heavy atoms (C, N, O) in the ligand structure. [d] Docking convergence: number of structures in the highest populated cluster, clustered with an RMSD value of 1 Å, out of 100 GA runs.

As discussed above (Figure 5), there are striking structural similarities in the side chains of the macrolides shown in Figure 2, all binding in an overlapping region with the gelsolin binding site. Consequently, the significance of the essential amino acids within this binding domain for the interactions

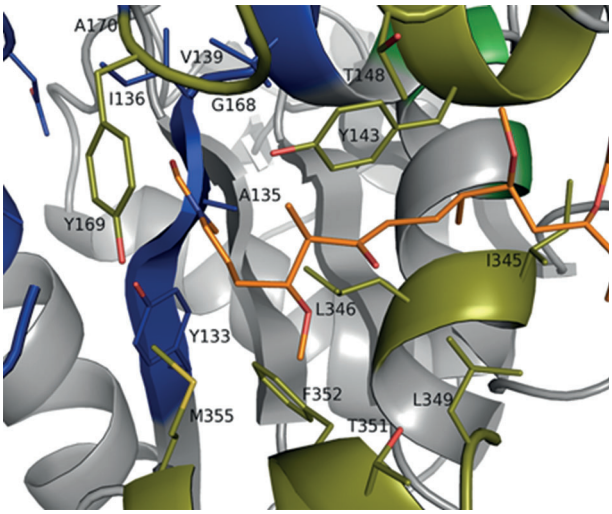

Figure 7. X-ray-derived position of the vinylformamide side chain of rhizopodin in the gelsolin binding pocket. The gelsolin binding pocket residues are shown in olive, those of the bistramide binding pocket in blue, and all others are in grey. The region of the docking site of the macrocyclic-type ligands is presented in green.

with the ligands from the crystal structures was analyzed in silico. For all structures, this revealed interactions of the vinylformamide side chain with residues G168, Y169, Y143, T148, I345, L346, L349, T351, F352, and M355 (Figure 7). In contrast, residues Y166 and T149 included in the gelsolin binding site are located at the outside of the cavity and are therefore not addressed by the smaller ligand side chains. However, the less bulky side chain of the ligands reaches further inside the pocket than gelsolin, resulting in additional interactions with residues Y133, I136, V139, A170, and F375[33] of the hydrophobic bistramide binding pocket. Interestingly, analysis of the ligand structures containing an amide function (either vinylformamide or simply amide) also revealed polar interactions with tyrosines Y143 and Y133, in agreement with the crystal structures.

Analogue design

Given the excellent potencies of bistramide and rhizopodin (see above), these two agents were selected for further analogue studies. It was envisioned that a particularly promising analogue would result from a combination of these two agents, in a rationale to address both the bistramide and the rhizopodin binding sites. Notably, these compounds present novel structural analogue types that are different from those previously reported. The previous analogues are based only on the macrocylic tail.[12f,26,27] Consequently, a common pharmacophore model was pursued, and simplified bistramide–rhizopodin hybrid structures were targeted.

As shown in Figure 8, three main fragments were differentiated during this analogue design. The first (fragment 1) would address the bistramide binding site only, the middle (fragment 2) would bind to the overlapping region, while the third (fragment 3) would target the internal rhizopodin pocket. Consequently, this strategy resulted in three different fragments: a bistramide-derived fragment, a fragment that represents the overlapping region, and a rhizopodin-derived fragment.

According to this strategy, different structural frameworks were docked into the binding pocket of the crystal structure of PDB ID: 1WUA. The position of the N1 atom in all crystal structures is highly conserved between the three tyrosines Y143, Y169, and Y133. Therefore, an amidic nitrogen was retained at this position (fragment 3, Figure 8). As chain extension, we chose the authentic side chain of rhizopodin (**11**), which lacks methyl groups at C4 and C12 relative to the other inhibitors with vinylformamide side chains (building block D). It was envisioned that fragments 1 and 2 should functionally address the back part of the cavity of the bistramide and the overlapping binding site, respectively (compare Figure 3 a,b with Figure 4). For this purpose, the middle part of the bistramide A ligand structure was directly retained (building block B) and slightly modified in order to evaluate the flexibility of this segment on

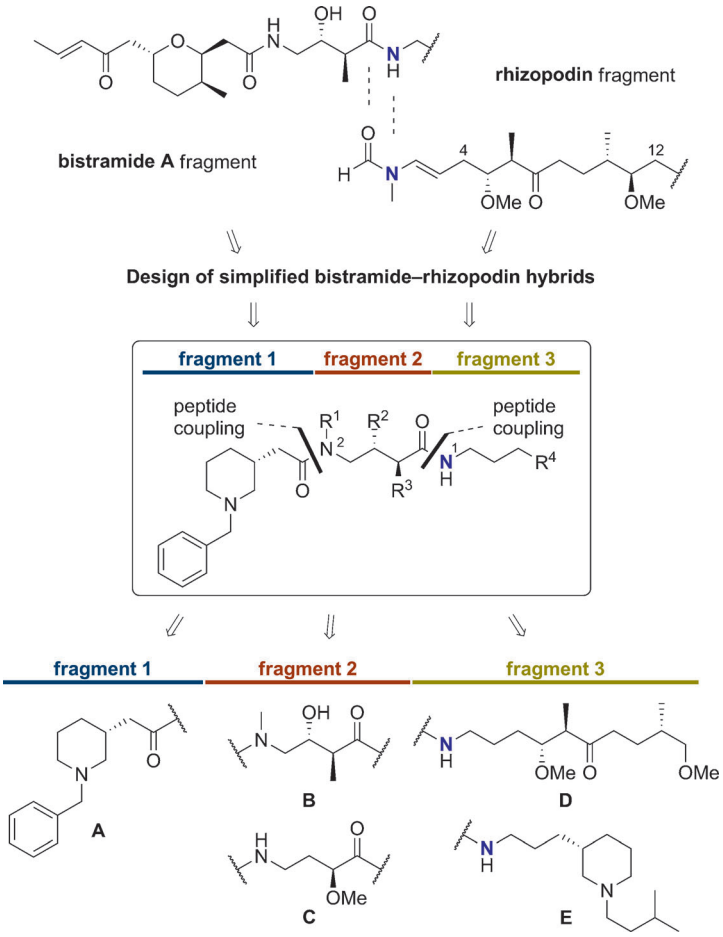

Figure 8. Design of simplified bistramide–rhizopodin hybrid structures based on a common pharmacophore model: template structure and modular building blocks.

the binding affinity. Concerning fragment 1, the tetrahydropyran was replaced by a simplified piperidine (building block A). In the crystal structure of actin-bound bistramide A, π–π interactions between the terminal enone and Y169 were observed. To retain this interaction, this fragment was terminated with a phenyl ring (building block A). Finally, we attempted to find a promising replacement for the side chain of rhizopodin. An overlay of the crystal structures of bistramide A and swinholide A, containing side chains that are different from rhizopodin, showed that a bulky aliphatic residue may effectively interact with the hydrophobic pocket consisting of T351, L346, F352, and M355. Therefore, in addition to the rhizopodin side chain D, building block E was also designed. This resulted in four rationally designed compounds with modular assemblies ABD, ACD, ABE, and ACE. The actin interactions of all of these compounds were calculated in a cross-docking approach with all available protein structures (see the Supporting Information for further details). The resulting binding energies of the highest populated clusters and the binding efficiencies with regard to the number of heavy atoms are summarized in Table 2.

All four analogues were predicted to show significantly improved binding efficiencies in the range of −0.41 to −0.46 kcal mol^{-1} as compared with rhizopodin and bistramide in connection with a decrease in the number of atoms. Interestingly, the sequences ABE and ACE with the simplified building blocks exhibit the highest binding efficiencies calculated: −0.45 and −0.46 kcal mol^{-1}. Replacement of the authentic side chain of rhizopodin (building block D, fragment 3) with the piperidine fragment (building block E, fragment 3) resulted in slightly improved binding efficiencies, which may suggest that the complex fragment of the rhizopodin structure may be replaced without loss of—or possibly even an increase in—potency. Replacement of the middle fragment (fragment 2) results in no significant energetic differences.

The reason behind the good binding efficiencies for the modular sequences ABE and ACE may be explained by the binding modes. As exemplarily shown in Figure 9 for **12**, the simplified analogue shows all the essential interactions for both the rhizopodin and bistramide binding sites. As anticipated, the N1 nitrogen is fixed between the three tyrosines Y143, Y169, and Y133. The piperidine with the appending aliphatic group of fragment 3 appears to fill the hydrophobic pocket consisting of L346, F352, T351, and M355. Fragment 1 likewise fits well into the hydrophobic pocket of the bistramide binding site and interacts with residues V139, P109, L110, and P112.

In summary, these modeling studies suggest that smaller side chain analogues may result in similar binding efficiencies as the 'barbed end' inhibitors if the template incorporates all essential interactions with the binding pocket of the protein. Based on the calculated effective increase in binding efficiencies, all analogues **12**–**15** should form good bases for the design of ligands with simplified core structures relative to the

Table 2. Binding energies and efficiencies of the rationally designed analogues of 'barbed end' actin inhibitors.[a]

Ligand	Sequence	E_{bind} [kcal mol^{-1}][b]	Binding Eff. [kcal mol^{-1}][c]	No. Heavy Atoms[d]
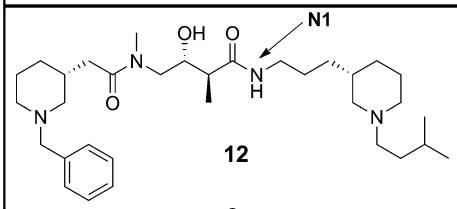 **12**	ABE	−17.8	−0.45	40
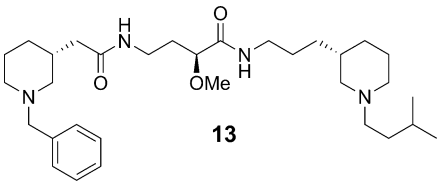 **13**	ACE	−18.1	−0.46	39
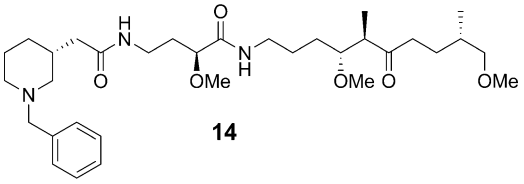 **14**	ABD	−17.2	−0.41	42
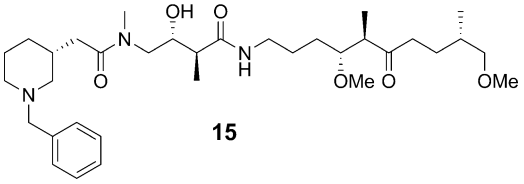 **15**	ACD	−18.3	−0.42	43

[a] Results from docking into the actin protein crystal structure (PDB ID: 1WUA). [b] Mean docked energy of all solutions in the highest populated cluster; the search area included 90 grid points in each dimension; 0.375 Å grid point distance; clustering by 1 Å RMSD. [c] Binding efficiency: E_{bind} divided by the number of heavy atoms. [d] Number of heavy atoms (C, N, O) in the ligand structure.

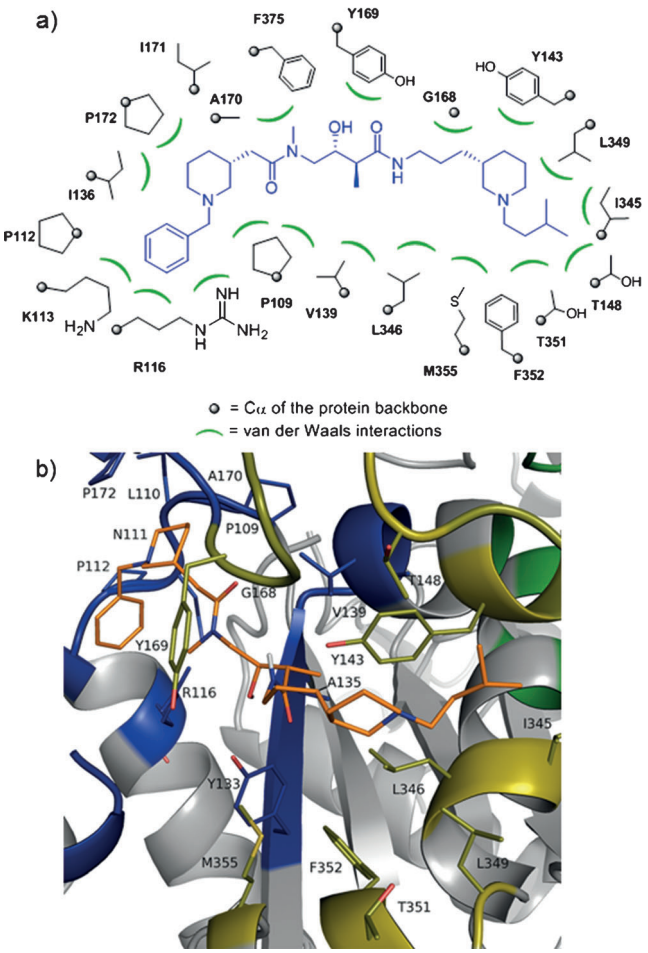

Figure 9. a) 2D and b) 3D presentations of the calculated position of the simplified hybrid analogue **12** with the fragment sequence (ABE) with actin. Shown is the cluster representative of the highest populated cluster.

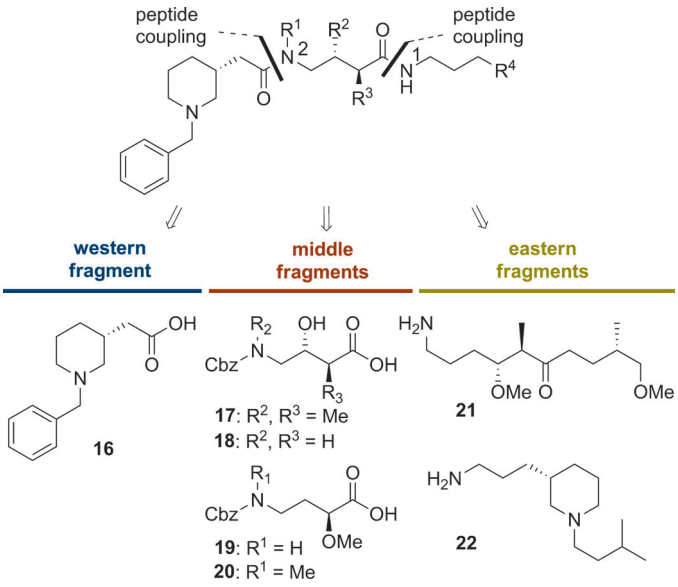

Figure 10. Retrosynthetic analysis.

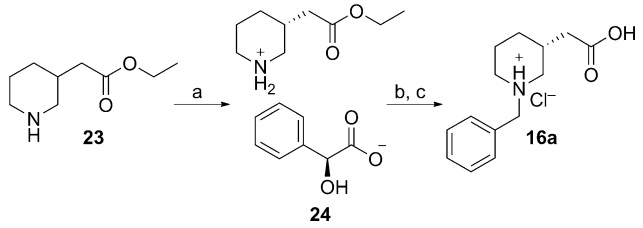

Scheme 1. Synthesis of western fragment **16a**. *Reagents and conditions*: a) *S*-(+)-mandelic acid, EtOAc, reflux, 36%; b) K_2CO_3, BnBr, acetone, RT, 87%; c) 6 M HCl, RT, 99%.

authentic natural products. In addition to the complete structures consisting of all three fragments, the evaluation of single or double fragments may also be instructive to delineate the minimum chain length required for biological potency. Importantly, this strategy is highly flexible and modular; each of these subunits can be readily replaced, thereby adding considerable flexibility to this approach.

Chemistry

As shown in Figure 10, the proposed hybrid analogues can be derived retrosynthetically from three main fragments: a western fragment (corresponding to fragment 1), a middle fragment (fragment 2), and an eastern fragment (fragment 3). These are linked by amide functionalities to enable rapid access to analogues for SAR studies.

Synthesis of the western fragment

As shown in Scheme 1, synthesis of the western fragment started from racemic ethyl 3-piperidinylacetate (**23**). Chiral resolution was achieved by fractional crystallization using the diastereomeric salts with *S*-(+)-mandelic acid according to published procedure.[34] Liberation of the amine was followed by benzylation[35] with benzyl bromide. Subsequent ester cleavage gave the desired compound **16** as its hydrochloride in nearly quantitative yield.

Synthesis of the middle fragments

For construction of the *anti*-propionate motif in the middle fragment **17**, a Masamune *anti*-aldol reaction with an appropriate aldehyde derived from amino alcohol **25** was chosen (Scheme 2).[36,37] The coupling proceeded in high diastereoselectivities and yields.[37] To allow facile liberation of the amine at a later stage of the synthesis by mild hydrogenolysis, installation of a benzyloxycarbonyl (Cbz) protecting group was necessary. After removal of the auxiliary of **26**, the *tert*-butoxycarbonyl (Boc) group was removed by using trifluoroacetic acid (TFA) before the Cbz group was installed by means of *N*-(benzyloxycarbonyloxy)succinimide (CbzOSuc), to afford acid **17**. The Cbz analogue of the aldehyde may also be used directly, but in this case the aldol reaction proceeded with considerably lower yields and diastereoselectivities.

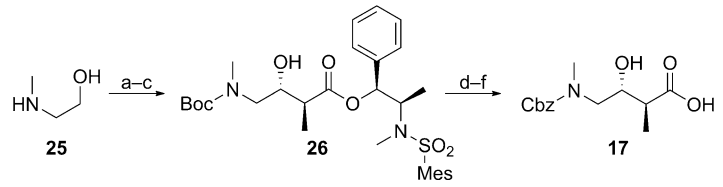

Scheme 2. Synthesis of compound **17**. *Reagents and conditions*: a) Boc_2O, Al_2O_3, neat, RT, 99%; b) IBX, EtOAc, reflux, 91%; c) Masamune's auxiliary, *c*Hex_2BOTf, Et_3N, CH_2Cl_2, −78 °C, 90%, d.r. = 96:4; d) NaOH, H_2O_2, *t*BuOH/MeOH, 0 °C, 99%; e) TFA, CH_2Cl_2, RT, 96%; f) CbzOSuc, $NaHCO_3$, acetone/H_2O, RT, 97%. IBX = 2-iodoxybenzoic acid, OTf = trifluoromethanesulfonate, Mes = mesityl.

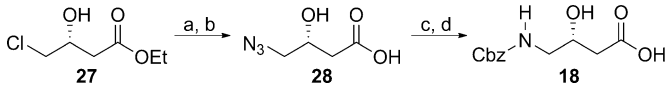

Scheme 3. Synthesis of compound **18**. *Reagents and conditions*: a) NaN_3, DMF, reflux, 85%; b) KOH, EtOH/H_2O, 97%; c) H_2, Pd/C, MeOH, RT, 96%; d) CbzOSuc, $NaHCO_3$, acetone/H_2O, RT, 96%.

Synthesis of amino acid **18** involved preparation of azide **28** from chloride **27** according to a sequence developed by Hayashi and co-workers (Scheme 3).[38] Azide introduction proceeded smoothly with sodium azide in *N*,*N*-dimethylformamide (DMF). Saponification of the ethyl ester gave **28**, which was further elaborated to the amino acid by hydrogenolysis in the presence of palladium on activated charcoal. For amine protection we relied again on a Cbz group, which was introduced in excellent yield under the conditions described above to give **18**.

Synthesis of the middle fragments **19** and **20** started from Cbz-protected amino acid **29** (Scheme 4). For O-methylation iodomethane and 2.0 equivalents of silver(I) oxide were used as a mild base to prevent racemization of the labile α-hydroxy moiety. Higher amounts of base also gave the N-methylated building block **31**, which can be separated by careful column chromatography. Finally, saponification of the methyl esters gave the desired compounds **19** and **20**.[39]

Synthesis of the eastern fragments

Efforts were next directed toward synthesis of the eastern fragment **21**, starting with a sequence previously developed in our research group during the course of the total synthesis of rhizopodin (**11**).[22c] We relied on a Masamune–Abiko aldol approach starting from aldehyde **32** (derived in two steps from 1,4-butanediol), to give an intermediate alcohol (not shown) in good yields as a single isomer after careful chromatographic separation (Scheme 5).[40,41]

After O-methylation, the auxiliary was replaced with *N*,*O*-dimethylhydroxylamine to give a Weinreb amide (not shown) in good yield following a procedure that was likewise developed in our research group.[42] Careful control of reaction conditions was crucial to avoid elimination of the methoxy group under the strongly basic reaction environment to give an enone byproduct, which proved inseparable

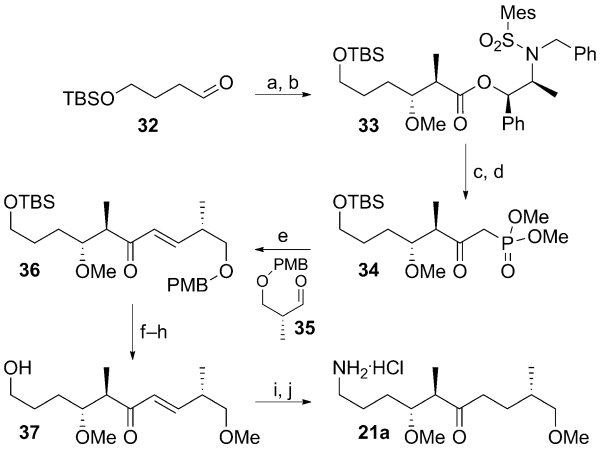

Scheme 5. Synthesis of compound **21**. *Reagents and conditions*: a) Masamune's auxiliary, *c*Hex_2BOTf, Et_3N CH_2Cl_2, −78 °C, 89%; b) MeI, Ag_2O, MS (3 Å), Et_2O, RT, 92%; c) CH_3NHOCH_3·HCl, *i*PrMgCl, THF, −15 °C→0 °C, 85%; d) $(MeO)_2P(O)Me$, *n*BuLi, THF, −78 °C, 93%; e) NaHMDS, THF, −78 °C→RT, 97%; f) DDQ, CH_2Cl_2/buffer (pH 7), 0 °C→RT, 97%; g) MeI, Ag_2O, MS (3 Å), Et_2O, RT, 96%; h) CSA, MeOH, RT, 97%; i) PPh_3, DIAD, DPPA, THF, 0 °C→RT, 86%; j) H_2, Pd/C, HCl/MeOH, RT. TBS = *tert*-butyldimethylsilyl, MS = molecular sieves, NaHMDS = sodium bis(trimethylsilyl)amide, DDQ = 2,3-dichloro-5,6-dicyano-*p*-benzoquinone, PMB = *para*-methoxybenzyl, CSA = camphorsulfonic acid, DIAD = diisopropyl azodicarboxylate, DPPA = diphenyl phosphoryl azide.

by column chromatography. To set stage for the Horner–Wadsworth–Emmons (HWE) reaction, the phosphonate moiety was introduced with dimethyl methylphosphonate to give compound **34**. The HWE reaction with *para*-methoxybenzyl (PMB)-protected Roche aldehyde **35**[43] gave **36** in excellent yields and exclusively as the *E* isomer, as determined from the ^{1}H NMR spectra. After PMB deprotection of **36** with 2,3-dichloro-5,6-dicyano-*p*-benzoquinone (DDQ), the liberated hydroxy function was methylated with a combination of iodomethane and silver(I) oxide. Alternatively, the O-methylated Roche aldehyde may also be used, but this resulted in considerably lower yields; therefore, this longer sequence was chosen. Finally, the primary *tert*-butyldimethylsilyl (TBS) group was removed under mildly acidic conditions. For introduction of the nitrogen, displacement of the terminal alcohol with an azide, bis-Boc-protected ammonia, or phthalimide were evaluated under Mitsunobu conditions.[44,45] From these alternatives, introduction of the azide worked

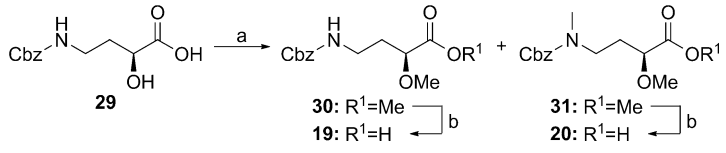

Scheme 4. Synthesis of compounds **19** and **20**. *Reagents and conditions*: a) MeI, Ag_2O, DMF, 5 °C, 78% (**30**/**31** = 1:3); b) NaOH, acetone/H_2O, RT, 97% (for **19**) and 99% (for **20**).

best, using diphenyl phosphoryl azide (DPPA) to give the desired azide (not shown).

At this stage, however, subsequent efforts to further advance this azide to **21** were thwarted by a seemingly impossible reduction of the azide moiety to the amine. Among the methods tested were the use of H_2, Pd/C, Staudinger conditions,[46] and Zn, NH_4Cl.[47] However, all of these methods led to decomposition or formation of a variety of undefined products. At this point we anticipated that the formed amine and the carbonyl group could undergo side reactions to prevent clean formation of **21**. Indeed, if the reaction was carried out under carefully controlled acidic conditions, leading to protonation of the amine, **21a** was formed in good yields, and the obtained crude hydrochloric acid salt was immediately subjected to amide couplings. Notably, the β-methoxy functionality again proved prone to elimination under these conditions, so that to some degree the eliminated product was formed.

For synthesis of the simplified eastern fragment **22**, (*R*)-(−)-3-piperidinecarboxylic acid (**38**) was identified as a suitable starting material, already containing the required stereogenic center (Scheme 6). Reduction[48] of the carboxylic acid yielded a primary alcohol (not shown), which was further elaborated

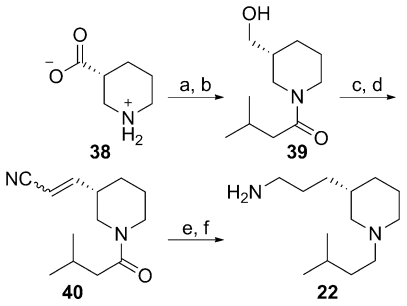

Scheme 6. Synthesis of compound **22**. *Reagents and conditions*: a) $LiAlH_4$, THF, reflux, 97%; b) isovaleric acid, DEPBT, Et_3N, THF, RT, 85%; c) IBX, EtOAc, reflux, 96%; d) $(EtO)_2P(O)CH_2CN$, NaHMDS, THF, −78 °C; e) H_2, Pd/C, MeOH, RT, 84% over two steps; f) $LiAlH_4$, THF, reflux, 84%. DEPBT = 3-(diethoxyphosphoryloxy)-1,2,3-benzotriazin-4(3*H*)-one.

by 3-(diethoxyphosphoryloxy)-1,2,3-benzotriazin-4(3*H*)-one (DEPBT)-mediated amide formation with isovaleric acid, which gave amide **39** exclusively without the competing formation of an ester.[49] In the next steps homologation and introduction of the nitrogen atom by HWE reaction was envisaged. Therefore, the primary alcohol had to be oxidized into an intermediate aldehyde, which was best performed with 2-iodoxybenzoic acid (IBX) in ethyl acetate at reflux.[50] The HWE reaction used diethyl cyanomethylphosphonate and sodium bis(trimethylsilyl)amide (NaHMDS) as base to give the desired α,β-unsaturated nitrile **40** in good yields with an *E*/*Z* ratio of 5:2.[51] The obtained mixture was then directly subjected to a double reduction sequence, first of the double bond to its saturated congener using hydrogen and palladium on activated charcoal, then of the nitrile and amide functionalities to the amines using lithium aluminum hydride, to give building block **22** in good yields over these two steps.[52]

Fragment union and completion of synthesis of the side chain analogues

As shown in Scheme 7, for fragment union, our strategy relied on DEPBT-mediated amide formation, which proceeded in a reliable manner. In detail, coupling of amine **22** with Cbz-protected amino acids **17**–**20** gave amides **41**–**44** in good yields (76–93%). For carbamate removal, palladium-catalyzed hydrogenation proved most efficient. Finally, for coupling of the liberated free amines with building block **16a**, addition of sodium carbonate as additional base was critical. Otherwise, considerably lower yields (35–53%) were obtained. In summary, following this sequence, the side chain analogues **12**, **13**, **45**, and **46** were prepared in a highly convergent manner over nine linear steps.

The synthesis of the side chain analogues **14**, **15**, **51**, and **52** was initiated by DEPBT-mediated amide formation of **21a** with **17**, **18**, **19**, and **20** to give **47**–**50** in pure form, after removal of elimination products by HPLC if required (Scheme 8). Cleavage of the protecting group by hydrogenolysis followed by DEPBT-mediated amide coupling with **16a** gave the desired products in good yields.

Biological results

For biological evaluation of the foregoing analogues, we first evaluated the inhibitory efficacy on the growth of the mammalian cervical carcinoma cell line KB-31 and the human mammary carcinoma cell line MCF-7. Both the final analogues (**12**–**15**,

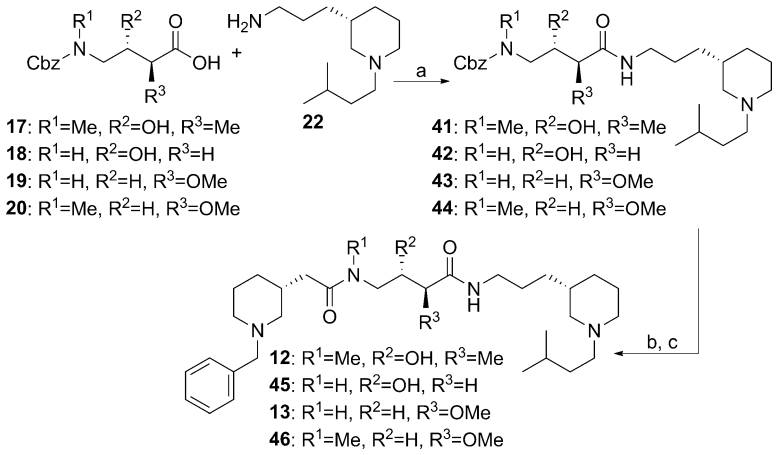

Scheme 7. Fragment union and formation of the side chain analogues **12**, **13**, **45**, and **46**. *Reagents and conditions*: a) DEPBT, Et_3N, THF, RT, 76–93%; b) H_2, Pd/C, MeOH, RT, 93–99%; c) **16a**, DEPBT, Et_3N, Na_2CO_3, THF, RT, 70–86%.

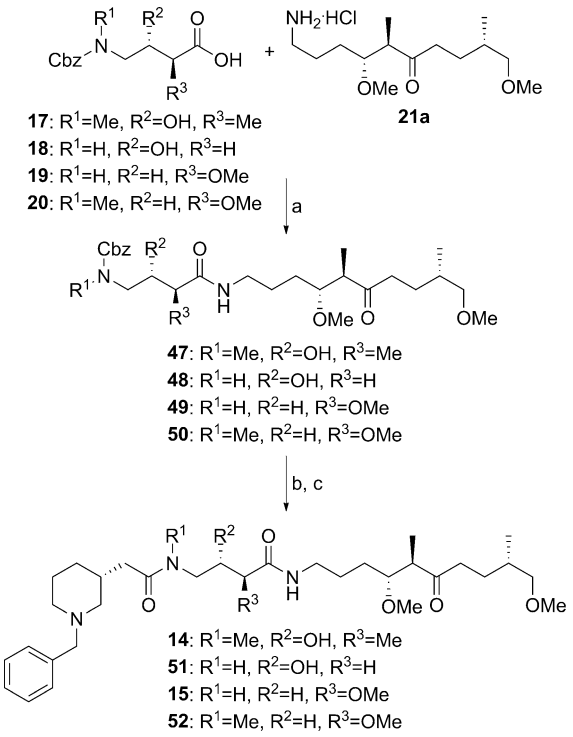

Scheme 8. Fragment union and formation of the side chain analogues **14**, **15**, **51**, and **52**. *Reagents and conditions*: a) DEPBT, Et_3N, Na_2CO_3, THF, RT, 57–62%; b) H_2, Pd/C, HCl, MeOH, RT, 91–95%; c) **16a**, DEPBT, Et_3N, Na_2CO_3, THF, RT, 70–78%.

45, **46**, **51**, and **52**) as well as the synthetic intermediates (**41**–**44** and **47**–**50**) were evaluated. As shown in Table 3, among all the novel ligands, three compounds (**49**, **50**, and **54**[56]) showed moderate activities, with IC_{50} values in the mid-micromolar range, and two further ligands (**48** and **53**[55]) showing effects at high micromolar concentrations. Notably, all the active compounds contained the original rhizopodin side chain, while the corresponding compounds bearing the simplified piperidine segments (**48** vs. **41**, **49** vs. **43**, and **50** vs. **44**) did not show any activity. The configuration at C10 had only a minor influence on the activity (**49** and **54**). None of the compounds that incorporated the piperidine substitute for the bistramide segment (i.e., fragment 1, see Figure 8) showed activity at the concentrations studied, suggesting the piperidine to be an unsuitable substitute. It is possible that the proposed fragment 1 may be too voluminous (compare **14**, **15**, **51**, and **52** with **48**–**50**, **53**, and **54**).

We then analyzed the effect of these compounds (i.e., **48**–**50**, **53**, and **54**) on the morphology of PtK_2 epithelial kidney cells derived from a male potoroo by fluorescence microscopy. As previously described,[17b] F-actin filaments were made visible with fluorescein isothiocyanate (FITC)-labeled phalloidin which binds specifically to polymerized actin. The cells were first treated with these compounds at concentrations of 25 $\mu g\,mL^{-1}$ (~50 μM), in direct comparison with rhizopodin. As shown in Figure 11 b, treatment of the cells with rhizopodin leads to a gradual decay of the stress fibers within minutes, relative to control cells (Figure 11 a), resulting in a complete restitution of F-actin.[17b] In contrast, the analogues did not cause any pronounced effects on the treated cells at these concentrations (e.g., **54**: Figure 11 c). Only for one of the compounds (i.e., **50**: Figure 11 d), a very weak effect at the border area of the cells may be visible, resulting in small knots in the cortex of the cells.[57]

Conclusions

In summary, we have developed an initial set of simplified hybrid analogues of the highly potent actin binding agents rhizopodin and bistramide, based on an interdisciplinary approach at the interface of molecular modeling, organic synthesis, and chemical biology. Computational analyses of noncovalent actin–inhibitor interactions were performed with AutoDock and the DrugScore scoring function, and were validated by re-docking of known actin binding ligands. This guided the design of a novel, highly modular and simplified class of hybrid analogues with a rationale to address both the bistramide and rhizopodin binding sites. Synthesis of these compounds was carried out by a highly modular and convergent three-fragment coupling strategy, enabling rapid access to dramatically simplified rhizopodin–bistramide hybrids. This new analogue class was analyzed for its antiproliferative and actin binding properties. Most analogues demonstrated only moderate or no antiproliferative or actin binding properties. However, a certain degree of antiproliferative activity was retained for analogues resembling the original side chain of rhizopodin. This may suggest that more elaborate and structurally related analogues may indeed retain the activity of the original natural products, in agreement with previous results from the Marriott[12f,26] and Nicolaou[24] research groups. These results also suggest that the in silico model may need further refinement. Furthermore, a broader set of SAR data will be helpful for delineation and simplification of the pharmacophore. In general, a more detailed theoretical understanding and predictive analysis of intermolecular noncovalent interactions in target–inhibitor studies for functional design is warranted.

Experimental Section

Computational details

To model the 'barbed end' of actin, the X-ray structures of actin with bound 'barbed end' inhibitors such as kabiramide C (1QZ5), jaspisamide A (1QZ6), ulapualide A (1S22), aplyronine A (1WUA), swinholide A (1YXQ), reidispongiolide A (2ASM), reidispongiolide C (2ASP), sphinxolide B (2ASO), bistramide A (2FXU), rhizopodin (2VYP), and lobophorolide (3M6G) were considered. All structures were aligned with the crystal structure of actin with bound aplyronine A (1WUA) in order to adjust the binding pockets. Crystallographic water molecules, metal ions, and cofactors were removed, as were alternative protein residues (Table S1, Supporting Information (SI)). Missing atoms located close to the ligand binding site were added manually, followed by a brief minimization with the molecular modeling package Macromodel 9.7,[58] constraining the rest of the structure to the X-ray coordinates. Processing the ligands was carried out by adding absent atoms followed by brief minimization (100 steps, OPLS2005 force field,[59] aqueous solution) of the added ligand part within the corresponding protein binding

Table 3. Inhibitory effects of ligands on the growth of the mammalian cervical carcinoma cell line KB-31 and human mammary carcinoma cell line MCF-7.[a,c]

Ligand[b]	MCF-7[a]		KB-31[b]	
	IC_{50} [μM]	IC_{90} [μM]	IC_{50} [μM]	IC_{90} [μM]
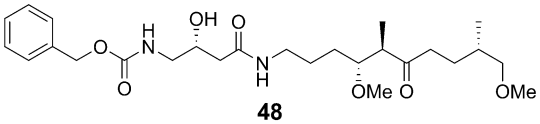 **48**	103.0 ± 29.0	> 370	27.5 ± 19.4	> 370
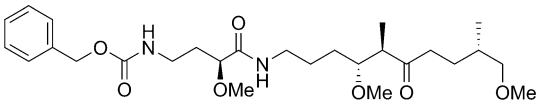 **49**	55.0 ± 39.0	370 ± 0.0	16.1 ± 16.2	> 370
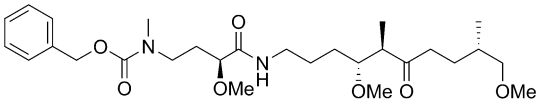 **50**	41.2 ± 0.0	350 ± 0.0	9.2 ± 0.0	> 370
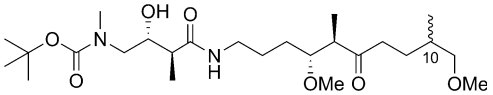 **53** (d.r. ~ 6:4)	123.5 ± 0.0	> 370	27.5 ± 0.0	> 370
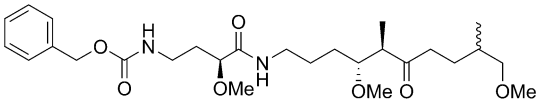 **54** (d.r. ~ 6:4)	61.9 ± 29.2	> 370	11.5 ± 3.2	> 370

[a] Cell lines were obtained from the German collection of Microorganisms and Cell Cultures (DSMZ). Growth inhibition was measured as previously described, and metabolic activity was determined after five days using the WST-1 assay. Data are the mean ± SD from experiments performed in duplicate.[53] [b] All other compounds showed no activity at concentrations up to 370 μM. [c] Rhizopodin shows activities in the low-nanomolar range toward similar cell lines.[54]

pocket to generate a sensible bond length (Table S2, SI). All other atoms were kept at the positions of the crystal structure. Processing the side chain hybrids was performed by drawing the structures in Maestro (including polar hydrogen atoms), followed by a brief minimization within the protein of reidispongiolide A (2ASM). All co-crystal structures of actin exhibit similar to nearly identical positions of the amino acid backbone for the binding site of the ligand macrocycle as well as in the binding pocket of the ligand side chain (Figure S1, SI). Thus, the conformation of actin in the crystal structures is considered as the low-energy binding conformation for the 'barbed end' inhibitors and was kept fixed to X-ray coordinates during docking. Docking was conducted with a combination of rigid protein structure and partly flexible ligand structure using AutoDock 3.0[30] with the DrugScore objective function.[31] This combination has proven reliable for binding mode prediction in a "re-docking" evaluation.[60] The number of flexible bonds in the ligand was determined automatically and checked for plausibility (Tables S3 and S4, SI). Default parameters were used, except for the number of GA runs, which was set to 100, the population size, which was set to 200, the number of generations, which was set to 50000, and the number of evaluations, which was set to 3×10^7. The length of the ligands in the crystal structure varies from 20.5 to 37.5 Å. However, the search area and the electrostatic map size was chosen to be a cube, centered on the ligand, with a space diagonal of ~58.5 Å (edge length 33.75 Å, 90 grid points, 0.375 Å grid point distance) to cover the size of all ligands (results are depicted in Table 1 and SI Figure S2). Furthermore, smaller cubes with a space diagonal of 39.3 Å (edge length 22.7 Å, 60 grid points, 0.375 Å grid point distance) as well as 48.7 Å (edge length 28.1 Å, 75 grid points, 0.375 Å grid point distance) were applied to evaluate the influence of the search area (results are depicted in Figures S3 and S4, SI). For the re-docking process, each ligand was docked 100 times to the actin structure of the cor-

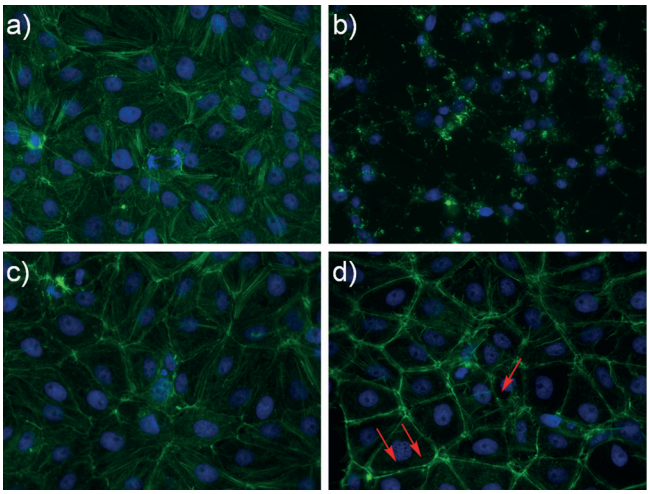

Figure 11. Fluorescence microscopy of PtK_2 cells after staining for F-actin (green); nuclei are blue: a) MeOH control 0.5%, b) rhizopodin 500 ng mL^{-1}, c) **54** 25 μg mL^{-1}, d) **50** 25 μg mL^{-1}.

responding co-crystal structure. Thus, 100 solutions were obtained for each ligand docking. The structures were clustered at a ligand RMSD of 1.0 Å. The highest populated clusters for each ligand were compared with the mean docked energy as well as the binding efficiency calculated with respect to the number of heavy atoms. The structure with lowest docking energy was regarded as cluster representative and was compared with the crystal structure (Tables S5 and S6, SI). To evaluate the docking results for various actin conformations, each ligand was docked onto each protein crystal structure in a cross-docking process. The results are summarized in Tables S7–S9, SI.

Synthesis details

Experimental details for the syntheses are given below. Please refer to the Supporting Information for the syntheses of compounds **32**–**34**, the Weinreb amide en route to **34**, as well as for the general methods.

Synthesis of the western fragment

Chiral resolution of amine 23. Synthesis was previously described.[34] This procedure gave **24** (36%) as a white solid; mp: 117 °C, $[\alpha]_D^{20} = +38.7^\circ$ ($c = 1.0$ in $CHCl_3$); ^{1}H NMR (500 MHz, $CDCl_3$): $\delta = 1.03$ (qd, $J = 12.4$, 4.7 Hz, 1H), 1.28 (t, $J = 7.1$ Hz, 3H), 1.51–1.65 (m, 2H), 1.74 (d, $J = 12.4$ Hz, 1H), 1.91–2.01 (m, 1H), 2.09–2.16 (m, 2H), 2.21 (td, $J = 12.4$, 4.4 Hz, 1H), 2.24 (t, $J = 12.0$ Hz, 1H), 2.97 (d, $J = 12.4$ Hz, 1H), 3.07 (d, $J = 12.0$ Hz, 1H), 4.14 (q, $J = 7.1$ Hz, 2H), 4.88 (s, 1H), 7.22 (t, $J = 7.4$ Hz, 1H), 7.29 (t, $J = 7.4$ Hz, 2H), 7.46 ppm (d, $J = 7.4$ Hz, 2H); ^{13}C NMR (125 MHz, $CDCl_3$): $\delta = 14.2$, 21.7, 28.5, 30.1, 38.0, 43.3, 47.6, 60.7, 74.4, 126.6, 127.1, 128.1, 142.5, 170.9, 178.9 ppm; HRMS-FAB m/z $[M]^+$ calcd for $C_9H_{18}NO_2^+$: 172.1332, found: 172.1341; d.r. ≥ 99:1%.[34b]

(3*R*)-1-Benzyl-3-(carboxymethyl)piperidin-1-ium chloride (16a): The salt **24** (208 mg, 0.642 mmol) was dissolved in 2 M Na_2CO_3 (5 mL). This solution was extracted with EtOAc (5×5 mL). The combined organic layers were dried over $MgSO_4$, filtered and concentrated in vacuo. The residue was dissolved in acetone (8 mL), and K_2CO_3 (488 mg, 3.53 mmol, 5.5 equiv) was added followed by benzyl bromide (103 μL, 0.706 mmol, 1.1 equiv). The mixture was stirred overnight at RT. Afterward the mixture was filtered and concentrated in vacuo. Purification by column chromatography (SiO_2, PE/*i*PrNH$_2$, 200:3) gave (*R*)-ethyl 2-(1-benzylpiperidin-3-yl)acetate as a colorless oil (146 mg, 87%): $R_f = 0.30$ (PE/*i*PrNH$_2$, 200:3); $[\alpha]_D^{20} = -2.2^\circ$ ($c = 1.0$ in $CHCl_3$); ^{1}H NMR (300 MHz, $CDCl_3$): $\delta = 0.89$–1.11 (m, 1H), 1.22 (t, $J = 7.2$ Hz, 3H), 1.54–1.70 (m, 2H), 1.70–1.83 (m, 2H), 2.00 (td, $J = 10.6$, 3.9 Hz, 1H), 2.04–2.17 (m, 1H), 2.19 (dd, $J = 14.6$, 6.5 Hz, 1H), 2.25 (dd, $J = 14.6$, 7.6 Hz, 1H), 2.68–2.82 (m, 2H), 3.49 (s, 2H), 4.10 (q, $J = 7.1$ Hz, 2H), 7.18–7.27 (m, 1H), 7.28–7.36 ppm (m, 4H); ^{13}C NMR (75 MHz, $CDCl_3$): $\delta = 14.2$, 24.8, 30.6, 33.2, 39.2, 53.9, 59.4, 60.2, 63.4, 126.8, 128.1, 129.0, 138.6, 172.7 ppm; HRMS-EI m/z $[M-H]^+$ calcd for $C_{16}H_{22}NO_2^+$: 260.1645, found: 260.1660.

(*R*)-Ethyl 2-(1-benzylpiperidin-3-yl)acetate (138 mg, 0.528 mmol) was dissolved in 6 M HCl (9.5 mL). The reaction mixture was stirred at RT for 4 h. Afterward the reaction mixture was concentrated in vacuo, co-evaporated with toluene (2×4 mL) to remove residual H_2O and finally dried in vacuo to give hydrochloride **16a** (141 mg, 99%) as a white crystalline solid; mp: 205 °C (dec.); $[\alpha]_D^{20} = +1.4^\circ$ ($c = 1.0$ in MeOH); ^{1}H NMR (500 MHz, CD_3OD): $\delta = 1.18$–1.38 (m, 1H), 1.78–2.01 (m, 3H), 2.22–2.41 (m, 3H), 2.80 (t, $J = 11.5$ Hz, 1H), 2.95 (t, $J = 11.6$ Hz, 1H), 3.44 (d, $J = 11.6$ Hz, 1H), 3.51 (d, $J = 11.5$ Hz, 1H), 4.34 (s, 2H), 7.44–7.52 (m, 3H), 7.52–7.61 ppm (m, 2H); ^{13}C NMR (125 MHz, CD_3OD): $\delta = 23.8$, 29.2, 32.6, 38.5, 53.6, 57.5, 62.1, 130.5, 130.6, 131.4, 132.6, 174.7 ppm; HRMS-ESI m/z $[M]^+$ calcd for $C_{14}H_{20}NO_2^+$: 234.1489, found: 234.1489.

Synthesis of the middle fragments

Masamune aldol reaction to form ester 26. *tert*-Butyl protection of **25** was previously described.[36] Following this procedure gave 2-[*N*-(*tert*-butyloxycarbonyl)-*N*-methylamino]ethanol (99%) as a colorless oil: $R_f = 0.25$ (PE/EtOAc, 6:4); ^{1}H NMR (300 MHz, $CDCl_3$): $\delta = 1.47$ (s, 9H), 2.93 (s, 3H), 3.40 (t, $J = 5.3$ Hz, 2H), 3.76 ppm (t, $J = 5.3$ Hz, 2H); ^{13}C NMR (75 MHz, $CDCl_3$): $\delta = 28.3$, 35.3, 51.2, 61.0, 79.7, 155.8, 157.0* ppm;[61a] HRMS-ESI m/z $[M+Na]^+$ calcd for $C_8H_{17}NNaO_3^+$: 198.1101, found: 198.1096.

2-[*N*-(*tert*-Butyloxycarbonyl)-*N*-methylamino]ethanol (166 mg, 0.948 mmol, 1.0 equiv) was dissolved in EtOAc (7 mL) before IBX (796 mg, 2.84 mmol, 3.0 equiv) was added. The suspension was held at reflux for 4 h before it was filtered over a pad of silica gel. The solvent was removed in vacuo to yield *tert*-butyl methyl(2-oxoethyl)carbamate (149 mg, 91%) as a colorless oil: $R_f = 0.48$ (PE/EtOAc, 6:4); ^{1}H NMR (300 MHz, $CDCl_3$): $\delta = 1.46$ (s, 4.5H), 1.41 (s, 4.5H), 2.92 (s, 1.5H), 2.94 (s, 1.5H), 3.90 (s, 1H), 4.00 (s, 1H), 9.59 ppm (s, 1H); ^{13}C NMR (75 MHz, $CDCl_3$): $\delta = 28.2$, 35.8, 58.7, 59.1*, 80.4, 80.6*, 155.3, 156.0*, 198.5 ppm;[61a] HRMS-ESI m/z $[M+Na]^+$ calcd for $C_8H_{15}NNaO_3^+$: 196.0944, found: 196.0940.

Masamune aldol reaction to form ester **26** was previously described.[37] Following this procedure gave **26** (90%, d.r. = 96:4) as a colorless oil: $R_f = 0.27$ (PE/EtOAc, 7:3); $[\alpha]_D^{20} = +8.3^\circ$ ($c = 0.8$ in $CHCl_3$); ^{1}H NMR (300 MHz, $CDCl_3$): $\delta = 1.18$ (d, $J = 7.4$ Hz, 3H), 1.31 (d, $J = 6.9$ Hz, 3H), 1.45 (s, 9H), 2.30 (s, 3H), 2.43 (s, 6H), 2.56–2.69 (m, 1H), 2.78 (s, 3H), 2.91 (s, 3H), 3.15–3.47 (m, 2H), 3.82–3.96 (m, 1H), 3.96–4.16 (m, 1H), 5.77 (d, $J = 5.5$ Hz, 1H), 6.87 (s, 2H), 6.97–7.11 (m, 2H), 7.11–7.25 ppm (m, 3H); ^{13}C NMR (75 MHz, $CDCl_3$): $\delta = 12.3$, 13.3, 20.9, 22.6, 28.3, 28.4, 36.2, 43.9, 52.9, 55.5, 72.8, 78.1, 80.1, 126.1, 128.0, 128.4, 131.9, 132.2, 138.0, 140.4, 142.3, 157.6, 173.8 ppm; HRMS-ESI m/z $[M+H]^+$ calcd for $C_{30}H_{45}N_2O_7S^+$: 577.2942, found: 577.2938.

(2*S*,3*R*)-4-(((Benzyloxy)carbonyl)(methyl)amino)-3-hydroxy-2-methylbutanoic acid (17). Saponification of **26** was previously described.[37] Following this procedure gave (2*S*,3*R*)-4-((*tert*-butoxycarbonyl)(methyl)amino)-3-hydroxy-2-methylbutanoic acid (99%) as a colorless oil: $R_f = 0.29$ (CH_2Cl_2/MeOH, 7:3); $[\alpha]_D^{20} = +2.3^\circ$ ($c = 1.0$ in $CHCl_3$); ^{1}H NMR (300 MHz, $CDCl_3$): $\delta = 1.26$ (d, $J = 7.0$ Hz, 3H), 1.45 (s, 9H), 2.58 (quint., $J = 7.0$ Hz, 1H), 2.93 (s, 3H), 3.14–3.38 (m, 1H), 3.38–3.57 (m, 1H), 3.85–3.97 (m, 1H), 5.92 ppm (br s, 2H); ^{13}C NMR (75 MHz, $CDCl_3$): $\delta = 13.8$, 28.3, 36.1, 43.2, 53.1, 72.5, 80.7, 157.7, 178.3 ppm; HRMS-ESI m/z $[M+K]^+$ calcd for $C_{11}H_{21}KNO_5^+$: 286.1051, found: 286.1052.

(2*S*,3*R*)-4-((*tert*-Butoxycarbonyl)(methyl)amino)-3-hydroxy-2-methylbutanoic acid (153 mg, 0.617 mmol, 1.0 equiv) was dissolved in CH_2Cl_2 (16 mL) at RT. TFA (0.95 mL, 12.3 mmol, 20 equiv) was added and the mixture was stirred for 90 min. Afterward the volatiles were removed in vacuo and the residue was co-evaporated with toluene (2×5 mL) to give crude (2*R*,3*S*)-3-carboxy-2-hydroxy-*N*-methylbutan-1-aminium trifluoroacetate as a colorless gum (154 mg, 96%), which was used directly without further purification.

Crude (2*R*,3*S*)-3-carboxy-2-hydroxy-*N*-methylbutan-1-aminium trifluoroacetate (154 mg, 0.590 mmol, 1.0 equiv) was dissolved in acetone/H_2O (1:1 *v*/*v*, 2 mL) at RT before $NaHCO_3$ (198 mg, 2.36 mmol, 4.0 equiv) was added followed by CbzOSuc (166 mg, 0.666 mmol

1.1 equiv). The reaction mixture was stirred for two days before it was diluted with H_2O (4 mL) and acetone was removed in vacuo. The aqueous layer was washed with CH_2Cl_2 (2×3 mL) before it was acidified with 1 M HCl to pH 3. Afterward it was extracted with EtOAc (4×5 mL). The combined organic layers were washed with H_2O (1×4 mL) and brine (1×4 mL), dried ($MgSO_4$) and concentrated to yield **17** (161 mg, 97%) as a colorless oil: R_f=0.73 (CH_2Cl_2/MeOH, 9:1); $[\alpha]_D^{20}=-2.6^\circ$ (c=1.0 in $CHCl_3$); ^{1}H NMR (300 MHz, CD_3OD): δ=1.10 (d, J=7.0 Hz, 1.5H), 1.19 (d, J=7.0 Hz, 1.5H), 2.44–2.59 (m, 1H), 3.00 (s, 1.5H), 3.02 (s, 1.5H), 3.15–3.30 (m, 1H), 3.47–3.62 (m, 1H), 3.90–4.01 (m, 1H), 5.11 (s, 2H), 7.25–7.44 ppm (m, 5H); ^{13}C NMR (75 MHz, CD_3OD): δ=13.9, 14.0*, 36.5, 36.9*, 45.5, 53.8, 54.3*, 68.5, 72.9, 73.1*, 128.9, 129.1*, 129.2, 129.6, 138.3, 158.3, 158.6*, 178.2 ppm;[61a] HRMS-ESI m/z $[M-H]^-$ calcd for $C_{14}H_{18}NO_5^-$: 280.1190, found: 280.1182.

(*R*)-4-Azido-3-hydroxybutanoic acid (28). Synthesis was previously described.[38] Following this procedure gave (*R*)-ethyl 4-azido-hydroxybutanoate (85%) as a yellow oil: R_f=0.24 (PE/EtOAc, 3:1); $[\alpha]_D^{20}=+15.6^\circ$ (c=1.0 in $CHCl_3$); ^{1}H NMR (400 MHz, $CDCl_3$): δ=1.29 (t, J=7.2 Hz, 3H), 2.52 (dd, J=16.6, 4.8 Hz, 1H), 2.57 (dd, J=16.6, 7.6 Hz, 1H), 2.96 (br s, 1H), 3.33 (dd, J=12.6, 5.9 Hz, 1H), 3.38 (dd, J=12.6, 4.4 Hz, 1H), 4.19 (q, J=7.2 Hz, 2H) 4.21 ppm (dddd, J=7.6, 5.9, 4.8, 4.4 Hz, 1H); ^{13}C NMR (100 MHz, $CDCl_3$): δ=14.1, 38.4, 55.5, 61.0, 67.3, 172.1 ppm; HRMS-ESI m/z $[M+Na]^+$ calcd for $C_6H_{11}N_3NaO_3^+$: 196.0693, found: 196.0697.

Saponification of (*R*)-ethyl 4-azido-hydroxybutanoate was previously described.[38] Following this procedure gave **28** (97%) as a colorless oil: R_f=0.53 (CH_2Cl_2/MeOH, 9:1); $[\alpha]_D^{20}=+22.4^\circ$ (c=0.5 in CH_2Cl_2); ^{1}H NMR (400 MHz, $CDCl_3$): δ=2.60 (dd, J=16.8, 4.8 Hz, 1H), 2.65 (dd, J=16.8, 7.8 Hz, 1H), 3.38 (dd, J=12.6, 6.2 Hz, 1H), 3.43 (dd, J=12.6, 4.4 Hz, 1H), 4.24 (dddd, J=7.8, 6.2, 4.8, 4.4 Hz, 1H), 6.53 ppm (br s, 2H); ^{13}C NMR (75 MHz, $CDCl_3$): δ=38.3, 55.5, 67.1, 176.8 ppm; HRMS-ESI m/z $[M-H]^-$ calcd for $C_4H_6N_3O_3^-$: 144.0415, found: 144.0414.

(*R*)-4-(((Benzyloxy)carbonyl)amino)-3-hydroxybutanoic acid (18). To a stirred solution of azide **28** (1.26 g, 8.69 mmol) in MeOH (225 mL) Pd/C (10%, 900 mg) was added. The resulting reaction mixture was stirred for 2 h under an atmosphere of H_2. Afterward, the reaction mixture was filtered through a pad of Celite which was rinsed thoroughly with MeOH (600 mL) and finally with H_2O (600 mL). The resulting filtrate was concentrated in vacuo to yield (*R*)-4-amino-3-hydroxybutanoic acid (993 mg, 96%) as a colorless solid: R_f=0.27 (*n*-butanol/acetic acid/H_2O, 4:1:1); mp: 213 °C (dec.); $[\alpha]_D^{20}=-17.4^\circ$ (c=1.0 in H_2O); ^{1}H NMR (400 MHz, D_2O): δ=2.41 (d, J=6.5 Hz, 2H), 2.93 (dd, J=13.0, 9.5 Hz, 1H), 3.14 (dd, J=13.0, 3.2 Hz, 1H), 4.18 ppm (dtd, J=9.5, 6.5, 3.2 Hz, 1H); ^{13}C NMR (75 MHz, D_2O): δ=44.3, 46.2, 68.0, 180.7 ppm; HRMS-ESI m/z $[M+Na]^+$ calcd for $C_4H_9NNaO_3^+$: 142.0475, found: 142.0478.

Cbz protection of (*R*)-4-amino-3-hydroxybutanoic acid was performed following the procedure for compound **17**. Cbz-protected amino acid **18** (96%) was obtained as a colorless oil: R_f=0.58 (CH_2Cl_2/MeOH, 9:1); $[\alpha]_D^{20}=+2.3^\circ$ (c=1.0 in $CHCl_3$); ^{1}H NMR (400 MHz, CD_3OD): δ=2.35 (dd, J=15.6, 8.5 Hz, 1H), 2.49 (dd, J=15.6, 4.3 Hz, 1H), 3.17 (dd, J=13.8, 6.6 Hz, 1H), 3.22 (dd, J=13.8, 5.3 Hz, 1H), 4.04–4.12 (m, 1H), 5.08 (s, 2H), 7.26–7.40 ppm (m, 5H); ^{13}C NMR (75 MHz, CD_3OD): δ=40.6, 47.5, 67.7, 68.7, 129.0, 129.1, 129.6, 138.4, 159.2, 175.3 ppm; HRMS-ESI m/z $[M-H]^-$ calcd for $C_{14}H_{18}NO_5^-$: 252.0877, found: 252.0869.

(*S*)-Methyl 4-(((benzyloxy)carbonyl)amino)-2-methoxybutanoate (30) and (*S*)-methyl 4-(((benzyloxy)carbonyl)(methyl)amino)-2-methoxybutanoate (31). (*S*)-(+)-*Z*-4-Amino-2-hydroxybutyric acid (29) (1.00 g, 3.95 mmol, 1.0 equiv) was dissolved in dry DMF (10 mL) and cooled to 5 °C. Ag_2O (3.66 g, 15.8 mmol, 4.0 equiv) and iodomethane (2.5 mL, 39.5 mmol, 10 equiv) were added and the mixture was stirred overnight at 5 °C in the dark. Afterward, the reaction mixture was diluted with EtOAc and filtered over a plug of Celite. Next, all volatiles were removed in vacuo. Purification by column chromatography (SiO_2, PE/EtOAc, 3:1) gave **30** (201 mg, 18%) and **31** (698 mg, 60%) as colorless oils. **Data for 30**: R_f=0.16 (PE/EtOAc, 3:1); $[\alpha]_D^{20}=-15.0^\circ$ (c=0.5 in $CHCl_3$); ^{1}H NMR (300 MHz, $CDCl_3$): δ=1.87–2.08 (m, 2H), 3.25–3.39 (m, 2H), 3.40 (s, 3H), 3.75 (s, 3H), 3.86 (dd, J=7.7, 4.4 Hz, 1H), 5.10 (s, 3H), 7.28–7.41 ppm (m, 5H); ^{13}C NMR (75 MHz, $CDCl_3$): δ=32.6, 37.7, 52.0, 58.3, 66.6, 78.9, 128.1, 128.1, 128.5, 136.6, 156.3, 172.7 ppm; HRMS-ESI m/z $[M+H]^+$ calcd for $C_{14}H_{20}NO_5^+$: 282.1336, found: 282.1339. **Data for 31**: R_f=0.22 (PE/EtOAc, 3:1); $[\alpha]_D^{20}=-16.2^\circ$ (c=1.0 in $CHCl_3$); ^{1}H NMR (400 MHz, $CDCl_3$): δ=1.85–1.96 (m, 1H), 1.97–2.09 (m, 1H), 2.93 (s, 3H), 3.29–3.42 (m, 4H), 3.44–3.59 (m, 1H), 3.68–3.82 (m, 4H), 5.14 (s, 2H), 7.28–7.43 ppm (m, 5H); ^{13}C NMR (100 MHz, $CDCl_3$): δ=30.8, 31.2*, 34.4, 35.0*, 45.0, 45.8*, 51.9, 58.1, 67.0, 67.1*, 77.9, 78.1*, 127.8, 127.9, 128.4, 136.8, 156.2, 172.7, 172.8* ppm;[61a] HRMS-ESI m/z $[M+Na]^+$ calcd for $C_{15}H_{21}NNaO_5^+$: 318.1312, found: 318.1312.

(*S*)-4-(((Benzyloxy)carbonyl)(methyl)amino)-2-methoxybutanoic acid (20). Methyl ester **31** (544 mg, 1.84 mmol) was dissolved in a mixture of acetone and 1 M NaOH solution (6:1 *v/v*, 19 mL). The mixture was stirred at RT for 3.5 h before it was adjusted to pH ~7 by adding 1 M HCl and then acetone was removed in vacuo. The mixture was basified to pH 12 by adding 1 M NaOH solution before it was washed with Et_2O (1×3 mL) to remove traces of unreacted starting material. The basic aqueous phase was acidified to pH 3 by addition of 1 M HCl solution which caused formation of a white precipitate. The aqueous phase was extracted with EtOAc (3×5 mL). The combined organic layers were dried over $MgSO_4$, filtered and concentrated in vacuo to give **20** (512 mg, 99%) as a colorless oil: R_f=0.36 (CH_2Cl_2/MeOH, 19:1); $[\alpha]_D^{20}=-8.8^\circ$ (c=1.0 in $CHCl_3$); ^{1}H NMR (400 MHz, $CDCl_3$): δ=1.89–2.01 (m, 1H), 2.02–2.14 (m, 1H), 2.94 (s, 3H), 3.32–3.44 (m, 4H), 3.49–3.59 (m, 1H), 3.75–3.84 (m, 1H), 5.15 (s, 2H), 7.28–7.40 (m, 5H), 8.52 ppm (br s, 1H); ^{13}C NMR (100 MHz, $CDCl_3$): δ=30.2, 30.8*, 34.3, 35.0*, 45.0, 45.5*, 58.2, 67.3, 77.4, 78.1*, 127.9, 128.0, 128.5, 136.6, 156.4, 156.8*, 175.5, 176.1* ppm;[61a] HRMS-ESI m/z $[M-H]^-$ calcd for $C_{14}H_{18}NO_5^-$: 280.1190, found: 280.1181.

(*S*)-4-(((Benzyloxy)carbonyl)amino)-2-methoxybutanoic acid (19). Synthesis previously described.[39] Following the procedure for **20** gave **19** (97%) as a colorless oil: R_f=0.28 (CH_2Cl_2/MeOH, 19:1); $[\alpha]_D^{20}=-21.3^\circ$ (c=1.0 in $CHCl_3$); ^{1}H NMR (400 MHz, $CDCl_3$): δ=1.92–2.11 (m, 2H), 3.28–3.43 (m, 2H), 3.44 (s, 3H), 3.84–3.91 (m, 1H), 5.11 (s, 2H), 5.17 (br s, 1H), 7.30–7.34 (m, 1H), 7.35–7.40 ppm (m, 4H); ^{13}C NMR (75 MHz, $CDCl_3$): δ=32.4, 37.6, 58.4, 66.8, 78.5, 128.1, 128.1, 128.5, 136.4, 156.6, 175.9 ppm; HRMS-ESI m/z $[M+Na]^+$ calcd for $C_{13}H_{17}NNaO_5^+$: 290.0999, found: 290.0993.

Synthesis of the eastern fragments

Dimethyl-((3*R*,4*R*)-7-(*tert*-butyldimethylsilyloxy)-4-methoxy-3-methyl-2-oxoheptyl) phosphonate (34). To a cold (−78 °C) solution of dimethyl methylphosphonate (0.60 mL, 5.54 mmol, 2.3 equiv) in dry THF (4.3 mL) *n*BuLi (1.6 M in hexanes, 3.3 mL, 5.30 mmol, 2.2 equiv) was added dropwise over a period of 20 min and stirring was continued for 1.5 h at −78 °C. Afterward (2*R*,3*R*)-6-(*tert*-butyldimethylsilyloxy)-*N*,3-dimethoxy-*N*,2-dimethylhexanamide (803 mg, 2.41 mmol, 1.0 equiv) in THF (3 mL) was added dropwise over a period of 30 min. The reaction mixture was stirred for 2 h at

−78 °C before it was quenched by addition of saturated NH_4Cl solution (4 mL). The mixture was allowed to warm to RT and then Et_2O (20 mL) and H_2O (5 mL) were added. The organic layer was separated and the aqueous layer was extracted with Et_2O (2× 20 mL) and CH_2Cl_2 (3×20 mL). The combined organic layers were dried ($MgSO_4$) and the solvent was removed in vacuo. Purification by column chromatography (SiO_2, PE/EtOAc, 4:6) yielded **34** (889 mg, 93%) as a pale-yellow oil: R_f = 0.13 (PE/EtOAc, 3:7); $[\alpha]_D^{20}$ = −61.4° (*c* = 1.0 in $CHCl_3$); ^{1}H NMR (300 MHz, $CDCl_3$): δ = 0.04 (s, 6H), 0.88 (s, 9H), 1.01 (d, *J* = 6.8 Hz, 3H), 1.39–1.71 (m, 4H), 2.97–3.08 (m, 1H), 3.10 (dd, *J* = 22.3, 14.2 Hz, 1H), 3.25 (s, 3H), 3.32 (dd, *J* = 22.3, 14.2 Hz, 1H), 3.33–3.41 (m, 1H), 3.61 (t, *J* = 6.0 Hz, 2H), 3.76 (d, *J* = 1.1 Hz, 3H), 3.80 ppm (d, *J* = 1.1 Hz, 3H); ^{13}C NMR (75 MHz, $CDCl_3$): δ = −5.2, 12.6, 18.5, 26.1, 26.4, 27.3, 42.3 (d, *J* = 129.3 Hz), 50.0 (d, *J* = 1.9 Hz), 53.1 (t, *J* = 6.2 Hz, 2C), 57.6, 63.1, 83.3, 205.9 ppm (d, *J* = 6.2 Hz); HRMS-ESI *m/z* $[M+Na]^+$ calcd for $C_{17}H_{37}NaO_6PSi^+$: 419.1989, found: 419.1993.

(2*S*,6*R*,7*R*,*E*)-10-(*tert*-Butyldimethylsilyloxy)-7-methoxy-1-(4-methoxybenzyloxy)-2,6-dimethyldec-3-en-5-one (36). Phosphonate **34** (341 mg, 0.861 mmol, 1.1 equiv) was dissolved in dry THF (32 mL). After cooling to −78 °C, NaHMDS (1.0 M in THF, 0.78 mL, 0.780 mmol, 1.0 equiv) was added dropwise over a period of 15 min. Stirring was continued for 1 h at −78 °C. Afterward, aldehyde **35**[43] (163 mg, 0.783 mmol, 1.0 equiv) was added over a period of 20 min. The reaction mixture was stirred for 2 h at −78 °C and was then slowly allowed to warm to RT. The mixture was stirred overnight before it was quenched by addition of buffer (pH 7, 55 mL). Et_2O (75 mL) was added and the organic layer was separated. The aqueous layer was extracted with Et_2O (3×50 mL) and the combined organic extracts were dried over $MgSO_4$. The solvent was removed in vacuo. After purification by column chromatography (SiO_2, PE/EtOAc, 10:1) **36** was yielded (363 mg, 97%) as a colorless oil: R_f = 0.25 (PE/EtOAc, 8:1); $[\alpha]_D^{20}$ = −29.2° (*c* = 1.0 in $CHCl_3$); ^{1}H NMR (300 MHz, $CDCl_3$): δ = 0.04 (s, 6H), 0.89 (s, 9H), 1.00 (d, *J* = 7.1 Hz, 3H), 1.09 (d, *J* = 6.9 Hz, 3H), 1.38–1.66 (m, 4H), 2.64 (virt. sept., *J* = 6.6 Hz, 1H), 3.01 (virt. quint., *J* = 7.3 Hz, 1H), 3.26 (s, 3H), 3.34–3.43 (m, 2H), 3.46–3.51 (m, 1H), 3.61 (t, *J* = 6.0 Hz, 2H), 3.80 (s, 3H), 4.44 (s, 2H), 6.20 (dd, *J* = 15.9, 1.1 Hz, 1H), 6.80 (dd, *J* = 15.9, 7.1 Hz, 1H), 6.86 (d, *J* = 8.5 Hz, 2H), 7.24 ppm (d, *J* = 8.5 Hz, 2H); ^{13}C NMR (75 MHz, $CDCl_3$): δ = −5.1, 12.8, 16.3, 18.5, 26.1, 26.7, 27.9, 37.1, 47.2, 55.4, 57.8, 63.3, 72.9, 73.9, 82.4, 113.9, 129.2, 129.3, 130.4, 149.4, 159.3, 203.0 ppm; HRMS-ESI *m/z* $[M+Na]^+$ calcd for $C_{27}H_{46}NaO_5Si$: 501.3007, found: 501.3007.

(2*S*,6*R*,7*R*,*E*)-10-Hydroxy-1,7-dimethoxy-2,6-dimethyldec-3-en-5-one (37). PMB ether **36** (227 mg, 0.474 mmol, 1.0 equiv) was dissolved in a mixture of CH_2Cl_2 and buffer (pH 7, 12 mL, 10:1 *v/v*). The mixture was cooled to 0 °C and DDQ (161 mg, 0.711 mmol, 1.5 equiv) was added. The reaction mixture was stirred for 30 min at 0 °C before it was allowed to warm to RT and stirred for additional 90 min. Afterward the mixture was quenched with saturated $NaHCO_3$ solution (15 mL). The organic layer was separated and the aqueous layer was extracted with CH_2Cl_2 (3×10 mL). The combined organic layers were washed with brine (15 mL), dried over $MgSO_4$, filtered and concentrated in vacuo. Purification by column chromatography (SiO_2, PE/EtOAc, 3:1) yielded (2*S*,6*R*,7*R*,*E*)-10-((*tert*-butyldimethylsilyl)oxy)-1-hydroxy-7-methoxy-2,6-dimethyldec-3-en-5-one (166 mg, 97%) as a colorless oil: R_f = 0.25 (PE/EtOAc, 2:1); $[\alpha]_D^{20}$ = −41.1° (*c* = 1.0 in $CHCl_3$); ^{1}H NMR (300 MHz, $CDCl_3$): δ = 0.05 (s, 6H), 0.89 (s, 9H), 1.02 (d, *J* = 7.0 Hz, 3H), 1.10 (d, *J* = 6.9 Hz, 3H), 1.38–1.53 (m, 1H), 1.54–1.68 (m, 3H), 1.70 (br s, 1H), 2.56 (virt. sept., *J* = 6.8 Hz, 1H), 2.96–3.08 (m, 1H), 3.28 (s, 3H), 3.44–3.54 (m, 1H), 3.55–3.66 (m, 4H), 6.26 (dd, *J* = 15.8, 1.0 Hz, 1H), 6.78 ppm (dd, *J* = 15.8, 7.6 Hz, 1H); ^{13}C NMR (75 MHz, $CDCl_3$): δ = −5.3, 12.7, 15.6, 18.3, 25.9, 26.4, 27.7, 39.5, 47.2, 57.7, 63.1, 66.6, 82.4, 130.0, 148.6, 202.8 ppm; HRMS-ESI *m/z* $[M+H]^+$ calcd for $C_{19}H_{39}O_4Si^+$: 359.2612, found: 359.2612.

Molecular sieves (3 Å), Ag_2O (2.13 g, 9.20 mmol, 20 equiv), and iodomethane (2.2 mL, 34.5 mmol, 75 equiv) were added to a solution of alcohol (2*S*,6*R*,7*R*,*E*)-10-((*tert*-butyldimethylsilyl)oxy)-1-hydroxy-7-methoxy-2,6-dimethyldec-3-en-5-one (165 mg, 0.460 mmol, 1.0 equiv) in dry Et_2O (10 mL). The reaction mixture was stirred at RT and exclusion of light overnight. Afterward, the mixture was filtered through a pad of Celite and it was washed thoroughly with Et_2O (100 mL). The solution was concentrated in vacuo to yield (2*S*,6*R*,7*R*,*E*)-10-((*tert*-butyldimethylsilyl)oxy)-1,7-dimethoxy-2,6-dimethyl-dec-3-en-5-one (165 mg, 96%), as a colorless oil: R_f = 0.37 (PE/EtOAc, 3:1); $[\alpha]_D^{20}$ = −33.1° (*c* = 1.0 in $CHCl_3$); ^{1}H NMR (300 MHz, $CDCl_3$): δ = 0.05 (s, 6H), 0.90 (s, 9H), 1.01 (d, *J* = 7.0 Hz, 3H), 1.09 (d, *J* = 6.9 Hz, 3H), 1.41–1.68 (m, 4H), 2.57–2.70 (m, 1H), 3.02 (dq, *J* = 8.0, 7.0 Hz, 1H), 3.29 (s, 3H), 3.31–3.38 (m, 2H), 3.34 (s, 3H), 3.45–3.53 (m, 1H), 3.59–3.65 (m, 2H), 6.22 (dd, *J* = 15.8, 1.4 Hz, 1H), 6.83 ppm (dd, *J* = 15.8, 7.1 Hz, 1H); ^{13}C NMR (75 MHz, $CDCl_3$): δ = −5.3, 12.6, 16.1, 18.3, 25.9, 26.6, 27.8, 36.9, 47.2, 57.7, 58.9, 63.1, 76.6, 82.3, 129.1, 149.0, 202.8 ppm; HRMS-ESI *m/z* $[M+Na]^+$ calcd for $C_{20}H_{40}NaO_4Si^+$: 395.2588, found: 395.2589.

Camphorsulfonic acid (43.9 mg, 0.189 mmol, 0.3 equiv) was added to a solution of (2*S*,6*R*,7*R*,*E*)-10-((*tert*-butyldimethylsilyl)oxy)-1,7-dimethoxy-2,6-dimethyl-dec-3-en-5-one (235 mg, 0.630 mmol, 1.0 equiv) in MeOH (6.5 mL). The reaction mixture was diluted with EtOAc (65 mL) after 15 min. The mixture was washed with saturated $NaHCO_3$ solution (2×15 mL) and brine (15 mL). The organic layer was separated and the combined aqueous layers were extracted with EtOAc (2×30 mL). The combined organic layers were dried over $MgSO_4$, filtered and concentrated in vacuo. Purification by column chromatography (SiO_2, PE/EtOAc, 1:1) yielded **37** (158 mg, 97%) as a colorless oil: R_f = 0.34 (EtOAc); $[\alpha]_D^{20}$ = −36.6° (*c* = 1.0 in $CHCl_3$); ^{1}H NMR (300 MHz, $CDCl_3$): δ = 1.03 (d, *J* = 7.1 Hz, 3H), 1.09 (d, *J* = 6.7 Hz, 3H), 1.48–1.59 (m, 1H), 1.60–1.73 (m, 3H), 2.17 (br s, 1H), 2.57–2.71 (m, 1H), 3.11 (quint., *J* = 7.1 Hz, 1H), 3.31–3.36 (m, 2H), 3.32 (s, 3H), 3.34 (s, 3H), 3.55 (td, *J* = 7.1, 2.5 Hz, 1H), 3.60–3.71 (m, 2H), 6.22 (dd, *J* = 15.9, 1.2 Hz, 1H), 6.84 ppm (dd, *J* = 15.9, 7.1 Hz, 1H); ^{13}C NMR (75 MHz, $CDCl_3$): δ = 12.2, 16.1, 26.9, 28.0, 36.9, 46.5, 57.6, 58.9, 62.9, 76.6, 82.0, 128.9, 149.4, 202.6 ppm; HRMS-ESI *m/z* $[M+Na]^+$ calcd for $C_{14}H_{26}NaO_4^+$: 281.1723, found: 281.1726.

(4*R*,5*R*,9*S*,*E*)-4,10-dimethoxy-5,9-dimethyl-6-oxodec-7-en-1-aminium chloride (21a). Triphenylphosphine (70.5 mg, 0.269 mmol, 1.3 equiv) was dissolved in dry THF (0.8 mL) at 0 °C and DIAD (53 μL, 0.269 mmol, 1.3 equiv) was added. After stirring the reaction mixture for 15 min, alcohol **37** (53.0 mg, 0.205 mmol, 1.0 equiv) dissolved in dry THF (1.5 mL) was added followed by slow addition of DPPA (58 μL, 0.269 mmol, 1.3 equiv). The reaction mixture was stirred for 3 h in the cold (0 °C) and for an additional 1 h at RT, before the reaction mixture was adsorbed onto Celite and purified directly by flash column chromatography (SiO_2, PE/EtOAc, 8:1) to afford (2*S*,6*R*,7*R*,*E*)-10-azido-1,7-dimethoxy-2,6-dimethyldec-3-en-5-one as a colorless oil (50.1 mg, 86%): R_f = 0.49 (PE/EtOAc, 2:1); $[\alpha]_D^{20}$ = −53.4° (*c* = 1.0 in CH_2Cl_2); ^{1}H NMR (300 MHz, $CDCl_3$): δ = 1.05 (d, *J* = 7.1 Hz, 3H), 1.12 (d, *J* = 6.8 Hz, 3H), 1.41–1.57 (m, 1H), 1.58–1.79 (m, 3H), 2.59–2.75 (m, 1H), 3.08 (quint., *J* = 7.1 Hz, 1H), 3.26–3.40 (m, 4H), 3.33 (s, 3H), 3.37 (s, 3H), 3.53 (td, *J* = 7.1, 3.2 Hz, 1H), 6.25 (dd, *J* = 15.9, 1.1 Hz, 1H), 6.87 ppm (dd, *J* = 15.9, 7.1 Hz, 1H); ^{13}C NMR (75 MHz, $CDCl_3$): δ = 12.2, 16.1, 24.3, 27.5, 36.9, 46.8, 51.6, 57.8, 58.9, 76.6, 81.7, 128.8, 149.5, 202.3 ppm;

HRMS-ESI m/z $[M+Na]^+$ calcd for $C_{14}H_{25}N_3NaO_3^+$: 306.1788, found: 306.1790.

Pd/C (10%, 30.0 mg) was added to a stirred solution of (2*S*,6*R*,7*R*,*E*)-10-azido-1,7-dimethoxy-2,6-dimethyldec-3-en-5-one (57.9 mg, 0.204 mmol) in methanolic HCl (0.25 M, 12 mL). The resulting reaction mixture was stirred for 35 min under an atmosphere of H_2. Afterward, the reaction mixture was filtered through a PTFE syringe filter (Chromafil Xtra, PTFE-45/25 0.45 μm) that was washed with MeOH (3×5 mL). The resulting filtrate was quickly concentrated in vacuo and the residue was co-evaporated with MeOH (5 mL) and with MeCN (5 mL) to finally yield the crude amine as hydrochloride **21 a** (60.0 mg, max. 99%) which was used directly without further purification.

(*R*)-1-(3-Hydroxymethyl)piperidin-1-yl)-3-methylbutan-1-one (39). $LiAlH_4$ (992 mg, 26.1 mmol, 2.5 equiv) was suspended in dry THF (45 mL) at RT. The resulting mixture was held at reflux and (*R*)-piperidine-3-carboxylic acid (**38**) (1.35 g, 10.4 mmol, 1.0 equiv) was added in small portions to the hot suspension (*NOTE: violent reaction!*). The resulting reaction mixture was held at reflux for 5 h. Afterward it was cooled to 0 °C and H_2O (1.0 mL), aqueous NaOH solution (3 M, 1.0 mL) and further H_2O (1.0 mL) were added in this order with an interval of 5 min each to give a white precipitate. The mixture was filtered and the precipitate was washed with warm Et_2O (300 mL). The organic phase was dried over Na_2SO_4, filtered and concentrated in vacuo to yield (*R*)-piperidin-3-ylmethanol as a colorless liquid (1.16 g, 97%): R_f = 0.28 (CH_2Cl_2/MeOH/*i*PrNH$_2$, 70:30:3); $[\alpha]_D^{20} = +13.8°$ (c = 0.8 in $CHCl_3$); ^{1}H NMR (300 MHz, $CDCl_3$): δ = 1.09–1.21 (m, 1H), 1.40–1.55 (m, 1H), 1.59–1.83 (m, 3H), 2.31 (br s, 2H) 2.41 (dd, J = 11.9, 9.7 Hz, 1H), 2.58 (td, J = 11.4, 3.0 Hz, 1H), 2.97 (dt, J = 11.7, 3.9 Hz, 1H), 3.14 (dd, J = 11.9, 3.6 Hz, 1H), 3.44 (dd, J = 10.6, 6.7 Hz, 1H), 3.54 ppm (dd, J = 10.6, 5.5 Hz, 1H); ^{13}C NMR (75 MHz, $CDCl_3$): δ = 25.7, 27.8, 39.3, 46.8, 49.9, 66.1 ppm; HRMS-ESI m/z $[M+H]^+$ calcd for $C_6H_{14}NO^+$: 116.1070, found: 116.1069.

To a stirred solution of (*R*)-piperidin-3-ylmethanol (786 mg, 6.82 mmol, 1.0 equiv) in dry THF (60 mL) isovaleric acid (0.82 mL, 7.50 mmol, 1.1 equiv), Et_3N (4.7 mL, 34.1 mmol, 5.0 equiv) and DEPBT (3.06 g, 10.2 mmol, 1.5 equiv) were added. The resulting reaction mixture was stirred overnight, before Et_2O (35 mL) and a saturated solution of $NaHCO_3$ (30 mL) were added. After stirring for 15 min, the organic layer was separated and the aqueous layer was extracted with EtOAc (3×50 mL). The combined organic layers were dried ($MgSO_4$), filtered and concentrated in vacuo. The resulting residue was purified by column chromatography (SiO_2, PE/EtOAc/*i*PrNH$_2$, 50:50: 3) to yield **39** (1.15 g, 85%) as a colorless oil: R_f = 0.26 (PE/EtOAc/*i*PrNH$_2$, 50:50:3); $[\alpha]_D^{20} = -25.0°$ (c = 1.0 in $CHCl_3$); ^{1}H NMR (500 MHz, $CDCl_3$): δ = 0.92–0.97 (m, 6H), 1.18–1.25 (m, 0.5H), 1.34–1.50 (m, 1.5H), 1.62–1.73 (m, 1.5H), 1.74–1.84 (m, 1.5H), 2.04–2.14 (m, 1H), 2.17–2.27 (m, 2H), 2.69–2.75 (m, 0.5H), 2.86 (dd, J = 13.4 Hz, 10.2 Hz, 0.5H), 3.20 (dd, J = 13.2 Hz, 7.4 Hz, 0.5H), 3.29 (ddd, J = 13.2, 8.4, 3.6 Hz, 0.5H), 3.40–3.49 (m, 1.5H), 3.50–3.59 (m, 1H), 3.87 (dd, J = 13.2, 3.3 Hz, 0.5H), 3.89–3.93 (m, 0.5H), 4.33 (dt, J = 13.2, 3.7 Hz, 0.5H), 5.49 ppm (br s, 1H); ^{13}C NMR (125 MHz, $CDCl_3$): δ = 22.4*, 22.7, 22.8, 22.8*, 24.3*, 24.4, 25.8*, 25.8, 26.5, 27.3*, 37.4, 39.4*, 42.0, 42.4*, 44.4*, 47.2, 49.1*, 63.4, 65.0*, 171.2*, 171.8 ppm;[61a] HRMS-ESI m/z $[M+Na]^+$ calcd for $C_{11}H_{21}NNaO_2^+$: 222.1465, found: 222.1465.

(*R*)-3-(1-(3-Methylbutanoyl)piperidin-3-yl)acrylonitrile (40). To a stirred solution of **39** (409 mg, 2.05 mmol, 1.0 equiv) in EtOAc (20 mL) IBX (1.73 g, 6.16 mmol, 3.0 equiv) was added and the resulting mixture was heated at reflux for 2 h. After TLC indicated consumption of starting material **39**, the mixture was allowed to cool to RT, filtered and concentrated in vacuo. The resulting residue was quickly purified by column chromatography (SiO_2, PE/EtOAc, 1:1) to yield (*R*)-1-(3-methylbutanoyl)piperidine-3-carbaldehyde as a colorless oil (388 mg, 96%): R_f = 0.27 (PE/EtOAc, 1:1); $[\alpha]_D^{20} = -40.2°$ (c = 1.0 in $CHCl_3$); ^{1}H NMR (500 MHz, $CDCl_3$): δ = 0.92–1.00 (m, 6H), 1.48–1.60 (m, 1H), 1.66–1.82 (m, 2H), 1.91–2.00 (m, 0.6H), 2.05–2.17 (m, 1.4H) 2.17–2.23 (m, 1H), 2.24–2.29 (m, 1H), 2.39–2.49 (m, 1H), 3.12 (ddd, J = 12.8, 9.8, 2.6 Hz, 0.4H), 3.26 (ddd, J = 13.0, 9.6, 3.2 Hz, 0.6H), 3.39–3.50 (m, 1H), 3.58 (dt, J = 13.0, 4.7 Hz, 0.6H), 3.81 (dd, J = 13.7, 2.7 Hz, 0.4H), 4.01 (dt, J = 12.8, 4.1 Hz, 0.4H), 4.23 (dd, J = 13.4, 3.6 Hz, 0.6H), 9.68 (s, 0.4H), 9.71 ppm (s, 0.6H); ^{13}C NMR (125 MHz, $CDCl_3$): δ = 22.7, 24.0*, 24.0, 24.5, 24.8*, 25.6*, 25.7, 41.5, 41.8*, 42.0*, 42.1, 45.2*, 46.3, 48.0, 48.4*, 171.2*, 171.2, 202.1*, 202.2 ppm;[61b] HRMS-EI m/z $[M-H]^+$ calcd for $C_{11}H_{18}NO_2^+$: 196.1343, found: 196.1351.

To a cold (−78 °C) stirred solution of diethyl cyanomethylphosphonate (106 μL, 0.654 mmol, 1.6 equiv) in dry THF (15 mL), a solution of NaHMDS (1.0 M solution in THF, 0.61 mL, 0.610 mmol, 1.5 equiv) was slowly added over a period of 20 min at −78 °C. The resulting solution was stirred for further 90 min at −78 °C. Afterward, a solution of (*R*)-1-(3-methylbutanoyl)piperidine-3-carbaldehyde (80.6 mg, 0.409 mmol, 1.0 equiv) in dry THF (3 mL) was added over a period of 15 min via syringe pump. The reaction mixture was stirred for 3 h at −78 °C and afterward allowed to slowly warm to RT overnight. The reaction mixture was quenched by the addition of buffer (pH 7, 5 mL) and Et_2O (15 mL). The organic layer was separated and the aqueous layer was extracted with EtOAc (3×10 mL). The combined organic layers were dried ($MgSO_4$), filtered and concentrated in vacuo. The resulting product **40** was obtained as a mixture of *E* and *Z* isomers (*E*/*Z* = 5:2) and hydrogenated without further purification: R_f *Z* isomer = 0.37 (PE/EtOAc, 3:7), *E* isomer = 0.46 (PE/EtOAc, 3:7).

(*R*)-3-(1-Isopentylpiperidin-3-yl)propan-1-amine (22). To a stirred solution of crude **40** (max. 0.409 mmol) in MeOH (15 mL) Pd/C (10%, 30 mg) was added. The resulting reaction mixture was stirred for 2 h under an atmosphere of H_2. Afterward the reaction mixture was filtered through a pad of Celite, washed with MeOH (15 mL) and finally with EtOAc (30 mL). The resulting filtrate was concentrated in vacuo and purified by column chromatography (SiO_2, PE/EtOAc, 1:1) to yield (*S*)-3-(1-(3-methylbutanoyl)piperidin-3-yl)propanenitrile (76.4 mg, 84% over two steps) as a colorless oil: R_f = 0.39 (PE/EtOAc, 3:7); $[\alpha]_D^{20} = -15.9°$ (c = 0.8 in $CHCl_3$); ^{1}H NMR (500 MHz, $CDCl_3$): δ = 0.93–0.98 (m, 6H), 1.12–1.28 (m, 1H), 1.39–1.57 (m, 2H), 1.58–1.75 (m, 3H), 1.86–1.94 (m, 1H), 2.05–2.12 (m, 1H), 2.17–2.23 (m, 2H), 2.37–2.43 (m, 2H) 2.60–2.66 (m, 1H), 2.74 (dd, J = 13.2, 9.9 Hz, 0.35H), 3.10 (ddd, J = 13.5, 10.4, 3.0 Hz, 0.65H), 3.67 (dt, J = 13.5, 4.1 Hz, 0.65H), 3.75–3.82 (m, 0.35H), 4.20–4.23 (m, 0.65H), 4.45 ppm (dt, J = 12.8, 3.6 Hz, 0.35H); ^{13}C NMR (125 MHz, $CDCl_3$): δ = 14.7*, 14.7, 22.6, 22.7, 22.7*, 24.4*, 25.0, 25.7, 28.7, 28.9*, 30.1, 30.2*, 34.7, 35.8*, 42.0*, 42.1, 42.2*, 46.1, 46.5, 51.2*, 119.1*, 119.5, 170.8*, 171.0 ppm;[61c] HRMS-ESI m/z $[M+H]^+$ calcd for $C_{13}H_{23}N_2O^+$: 223.1805, found: 223.1082.

To a stirred suspension of $LiAlH_4$ (190 mg, 5.00 mmol, 4.0 equiv) in dry THF (4 mL) a solution of (*S*)-3-(1-(3-methylbutanoyl)piperidin-3-yl)propanenitrile (277 mg, 1.25 mmol, 1.0 equiv) in dry THF (8 mL) was added carefully at RT. The resulting reaction mixture was held at reflux for 3.5 h. After TLC indicated the consumption of starting material, Et_2O (12 mL) was added and the reaction mixture was cooled to 0 °C. H_2O (0.23 mL), aqueous NaOH solution (3 M, 0.23 mL) and further H_2O (0.70 mL) were added in this order with an interval of 5 min each to give a white precipitate. Finally, the

mixture was dried (Na_2SO_4), filtered, washed with Et_2O (50 mL) and concentrated in vacuo to yield **22** (223 mg, 84%) after purification by column chromatography (SiO_2, Et_2O/$iPrNH_2$, 100:5) as a colorless liquid: R_f = 0.21 (PE/EtOAc/$iPrNH_2$, 50:50:5); $[\alpha]_D^{20} = +3.3^\circ$ (c = 1.0 in $CHCl_3$); ^{1}H NMR (500 MHz, $CDCl_3$): δ = 0.80–0.86 (m, 1H), 0.89 (d, J = 6.6 Hz, 6H), 1.17–1.34 (m, 4H), 1.36–1.41 (m, 2H), 1.42–1.49 (m, 2H), 1.50–1.59 (m, 4H), 1.62–1.67 (m, 1H), 1.74–1.78 (m, 1H), 1.79–1.82 (m, 1H), 2.27–2.31 (m, 2H), 2.66 (t, J = 7.1 Hz, 2H), 2.84–2.87 ppm (m, 2H); ^{13}C NMR (125 MHz, $CDCl_3$): δ = 22.7, 22.8, 25.5, 26.9, 31.1, 31.2, 31.9, 36.0, 36.1, 42.5, 54.5, 57.7, 60.8 ppm; HRMS-ESI m/z $[M+H]^+$ calcd for $C_{13}H_{29}N_2^+$: 213.2325, found: 213.2324.

Fragment union

General procedure 1: coupling of fragment 22 with middle fragments 17–20 to give amides 41–44. The Cbz-protected γ-amino acid (1.15–1.25 equiv) and amine **22** were dissolved in dry THF (0.1 M) at RT. Et_3N was added (5 equiv with respect to the amino acid) followed by DEPBT (1.5 equiv with respect to the amino acid) and the mixture was stirred at RT overnight. Half-saturated $NaHCO_3$ solution was added, and it was stirred for 30 min before it was extracted with EtOAc (five times). The combined organic extracts were dried ($MgSO_4$) and concentrated in vacuo. The crude product was purified by column chromatography (SiO_2, 3% $iPrNH_2$ in PE/EtOAc) giving the desired amides.

Benzyl ((2*R*,3*S*)-2-hydroxy-4-((3-((*R*)-1-isopentylpiperidin-3-yl)-propyl)amino)-3-methyl-4-oxobutyl)(methyl)carbamate (41). The reaction was performed according to general procedure 1 with **22** (42.0 mg, 0.198 mmol, 1.0 equiv), and **17** (67.1 mg, 0.239 mmol, 1.2 equiv) to give **41** (72.7 mg, 77%) as a yellow oil: R_f = 0.37 (PE/EtOAc/$iPrNH_2$, 50:50:3); $[\alpha]_D^{20} = +6.2^\circ$ (c = 1.0 in CH_2Cl_2); ^{1}H NMR (400 MHz, $CDCl_3$): δ = 0.81–0.89 (m, 1H), 0.90 (d, J = 6.6 Hz, 6H), 1.20–1.36 (m, 5H), 1.36–1.49 (m, 3H), 1.49–1.71 (m, 6H), 1.71–1.80 (m, 1H), 1.82–1.96 (m, 1H), 2.17–2.42 (m, 3H), 2.82–2.95 (m, 2H), 3.01 (s, 3H), 3.07–3.35 (m, 3H), 3.41–3.61 (m, 1H), 3.68–3.83 (m, 1H), 4.31 (br s, 1H), 5.13 (s, 2H), 5.68 (br s, 0.2H), 6.54 (br s, 0.8H), 7.29–7.44 ppm (m, 5H); ^{13}C NMR (150 MHz, $CDCl_3$): δ = 15.9, 16.0*, 22.7, 22.7, 25.1, 26.8, 26.8, 30.9, 31.8, 35.5, 35.7, 35.9, 36.4*, 39.6, 42.7, 43.0*, 53.5*, 54.2, 54.3, 57.5, 60.4, 67.2*, 67.3, 73.0, 127.8, 128.1, 128.5, 136.5, 136.6*, 156.2*, 157.4, 175.2, 175.5* ppm;[61d] HRMS-ESI m/z $[M+H]^+$ calcd for $C_{27}H_{46}N_3O_4^+$: 476.3483, found: 476.3483.

Benzyl ((*R*)-2-hydroxy-4-((3-((*R*)-1-isopentylpiperidin-3-yl)propyl)-amino)-4-oxobutyl)carbamate (42). The reaction was performed according to general procedure 1 with **22** (47.3 mg, 0.223 mmol, 1.0 equiv), and **18** (69.8 mg, 0.276 mmol, 1.24 equiv) to give **42** (75.9 mg, 76%) as a colorless oil: R_f = 0.17 (PE/EtOAc/$iPrNH_2$, 50:50:3); $[\alpha]_D^{20} = +3.3^\circ$ (c = 1.0 in CH_2Cl_2); ^{1}H NMR (400 MHz, $CDCl_3$): δ = 0.77–0.86 (m, 1H), 0.88 (d, J = 6.6 Hz, 6H), 1.14–1.26 (m, 2H), 1.35–1.44 (m, 2H), 1.44–1.55 (m, 3H), 1.56–1.68 (m, 4H), 1.69–1.77 (m, 1H), 1.88 (td, J = 11.3, 2.3 Hz, 1H), 2.25–2.40 (m, 4H), 2.82–2.95 (m, 2H), 3.10–3.26 (m, 3H), 3.26–3.36 (m, 1H), 4.00–4.08 (m, 1H), 4.88 (br s, 1H), 5.07 (s, 2H), 5.63 (t, J = 5.7 Hz, 1H), 6.50 (t, J = 5.0 Hz, 1H), 7.28–7.36 ppm (m, 5H); ^{13}C NMR (100 MHz, $CDCl_3$): δ = 22.6, 22.6, 24.9, 26.5, 26.8, 30.7, 31.7, 35.2, 35.4, 39.6, 39.9, 46.2, 54.0, 57.4, 60.2, 66.7, 67.9, 127.9, 128.0, 128.4, 136.4, 157.1, 171.8 ppm; HRMS-ESI m/z $[M+H]^+$ calcd for $C_{25}H_{42}N_3O_4^+$: 448.3170, found: 448.3169.

Benzyl ((*S*)-4-((3-((*R*)-1-isopentylpiperidin-3-yl)propyl)amino)-3-methoxy-4-oxobutyl) carbamate (43). The reaction was performed according to general procedure 1 with **22** (44.3 mg, 0.209 mmol, 1.0 equiv), and **19** (64.1 mg, 0.240 mmol, 1.15 equiv) to give **43** (89.6 mg, 92%) as a yellow oil: R_f = 0.22 (PE/EtOAc/$iPrNH_2$, 80:20:3); $[\alpha]_D^{20} = -16.1^\circ$ (c = 1.0 in CH_2Cl_2); ^{1}H NMR (400 MHz, $CDCl_3$): δ = 0.79–0.88 (m, 1H), 0.90 (d, J = 6.6 Hz, 6H), 1.14–1.27 (m, 2H), 1.37–1.47 (m, 2H), 1.47–1.71 (m, 7H), 1.72–1.80 (m, 1H), 1.82–2.02 (m, 3H), 2.29–2.41 (m, 2H), 2.84–2.96 (m, 2H), 3.17–3.32 (m, 3H), 3.33–3.44 (m, 1H), 3.39 (s, 3H), 3.68 (dd, J = 6.4, 5.1 Hz, 1H), 5.09 (s, 2H), 5.12–5.20 (m, 1H), 6.60 (t, J = 5.5 Hz, 1H), 7.28–7.39 ppm (m, 5H); ^{13}C NMR (125 MHz, $CDCl_3$): δ = 22.7, 22.7, 25.1, 26.8, 27.0, 30.9, 31.8, 32.3, 35.5, 35.7, 37.5, 39.1, 54.2, 57.5, 58.4, 60.4, 66.6, 80.8, 128.0, 128.1, 128.5, 136.6, 156.3, 171.8 ppm; HRMS-ESI m/z $[M+H]^+$ calcd for $C_{26}H_{44}N_3O_4^+$: 462.3326, found: 462.3326.

Benzyl ((*S*)-4-((3-((*R*)-1-isopentylpiperidin-3-yl)propyl)amino)-3-methoxy-4-oxobutyl)(methyl)carbamate (44). The reaction was performed according to general procedure 1 with **22** (46.9 mg, 0.220 mmol, 1.0 equiv), and **20** (77.3 mg, 0.275 mmol, 1.25 equiv) to give **44** (85.0 mg, 81%) as a colorless oil: R_f = 0.30 (PE/EtOAc/$iPrNH_2$, 80:20:3); $[\alpha]_D^{20} = -16.4^\circ$ (c = 1.0 in CH_2Cl_2); ^{1}H NMR (400 MHz, $CDCl_3$): δ = 0.79–0.87 (m, 1H), 0.89 (d, J = 6.6 Hz, 6H), 1.11–1.28 (m, 2H), 1.36–1.45 (m, 2H), 1.45–1.70 (m, 7H), 1.71–1.79 (m, 1H), 1.80–1.93 (m, 2H), 1.93–2.10 (m, 1H), 2.31–2.39 (m, 2H), 2.82- 2.98(m, 2H), 2.91 (s, 3H), 3.13–3.32 (m, 4.5H), 3.37 (s, 1.5H), 3.41–3.68 (m, 2H), 5.11 (s, 2H), 6.43–4.56 (m, 0.5H), 6.60–6.73 (m, 0.5H), 7.28–7.42 ppm (m, 5H); ^{13}C NMR (100 MHz, $CDCl_3$): δ = 22.6, 22.7, 25.0, 26.8, 27.0, 30.3, 30.6*, 30.8, 31.7, 33.9, 34.6*, 35.4, 35.6, 39.1, 44.8, 45.1*, 54.1, 57.4, 58.1, 58.2*, 60.3, 66.9, 80.1, 127.7, 127.8, 128.4, 136.8, 156.1*, 156.2, 171.6*, 171.9 ppm;[61a] HRMS-ESI m/z $[M+H]^+$ calcd for $C_{27}H_{46}N_3O_4^+$: 476.3483, found: 476.3482.

General procedure 2: Cbz deprotection of amides 41–44. Pd/C (10%, 0.5 mg per 1.0 mg amide) was added to a stirred solution of Cbz-protected amides **41**–**44** in MeOH (7.0 mg mL^{-1}). The resulting reaction mixture was stirred for 90 min under an atmosphere of H_2. Afterward the reaction mixture was filtered through a PTFE syringe filter (Chromafil Xtra, PTFE-45/25 0.45 μm). The resulting filtrate was concentrated in vacuo to yield the crude amines (93–99%), which were used directly without further purification.

General procedure 3: coupling of amines with western fragment 16a. To a stirred suspension of Na_2CO_3 (5.0 equiv), carboxylic acid (1.2 to 1.7 equiv) and crude amine (1.0 equiv) in dry THF (0.1 M) Et_3N (5.0 equiv) and DEPBT (2.0 equiv) were added. The resulting reaction mixture was stirred at RT overnight. After TLC indicated consumption of the amine, half-saturated $NaHCO_3$ solution was added and the mixture was stirred for 30 min before it was extracted with EtOAc (five times). The combined organic layers were dried over $MgSO_4$, filtered and concentrated in vacuo. The crude product was purified by column chromatography (SiO_2, 3% $NEtMe_2$ or $iPrNH_2$ in PE/EtOAc) to give the desired side chain analogues **12**–**15, 45, 46, 51** and **52**.

(2*S*,3*R*)-4-(2-((*R*)-1-Benzylpiperidin-3-yl)-*N*-methylacetamido)-3-hydroxy-*N*-(3-((*R*)-1-isopentylpiperidin-3-yl)propyl)-2-methylbutanamide (12). The reaction was performed according to general procedure 3 with acid **16a** (27.1 mg, 100 μmol, 1.12 equiv), and crude amine (derived from amide **41**, max. 89.0 μmol, 1.0 equiv) to give **12** (37.6 mg, 76%) as a colorless oil: R_f = 0.27 (EtOAc/$iPrNH_2$, 100:5); $[\alpha]_D^{20} = +7.7^\circ$ (c = 1.0 in CH_2Cl_2); ^{1}H NMR (400 MHz, $CDCl_3$): δ = 0.79–0.87 (m, 1H), 0.89 (d, J = 6.6 Hz, 6H), 0.97–1.09 (m, 1H), 1.12–1.25 (m, 2H), 1.25 (d, J = 7.1 Hz, 2.7H), 1.29 (d, J = 7.2 Hz, 0.3H), 1.36–1.44 (m, 2H), 1.48–1.69 (m, 9H), 1.71–1.79 (m, 2H), 1.79–1.88 (m, 2H), 2.03 (m, 1H), 2.10–2.25 (m, 2H), 2.25–2.36 (m, 4H), 2.64–2.72 (m, 1H), 2.76 (d, J = 9.5 Hz, 1H), 2.81–2.91 (m, 2H), 2.92 (s, 0.3H), 3.06 (s, 2.7H), 3.17–3.28 (m, 3H), 3.40–3.54 (m, 2H), 3.58–3.65 (m, 1H), 3.66–3.72 (m, 0.9H), 3.75–3.82 (m, 0.1H), 4.58

(br s, 1H), 6.26 (br s, 0.1H). 6.74 (t, $J=4.3$ Hz, 0.9H), 7.19–7.27 (m, 1H), 7.28–7.35 ppm (m, 4H); ^{13}C NMR (100 MHz, $CDCl_3$): $\delta=15.7$, 22.7, 22.7, 24.7, 25.3, 26.9, 26.9, 30.8, 31.0, 31.9, 33.0, 34.3*, 35.7, 35.8, 37.6, 37.9, 39.6, 41.2*, 43.5, 53.9, 53.9, 54.3, 57.6, 59.7, 60.5, 63.4, 71.6*, 73.2, 126.9, 128.1, 129.0, 129.1*, 138.5, 172.6*, 173.8, 175.0, 175.2* ppm;[61e] IR (film): $\tilde{\nu}=3310$, 2930, 2362, 1635, 1542, 1456, 732, 699 cm^{-1}; HRMS-ESI m/z $[M+Na]^+$ calcd for $C_{33}H_{56}N_4NaO_3^+$: 579.4245, found: 579.4242.

(*R*)-4-(2-((*R*)-1-Benzylpiperidin-3-yl)acetamido)-3-hydroxy-*N*-(3-((*R*)-1-isopentylpiperidin-3-yl)propyl)butanamide (45). The reaction was performed according to general procedure 3 with acid **16a** (29.6 mg, 110 μmol, 1.10 equiv), and crude amine (derived from amide **42**, max. 94.4 μmol, 1.0 equiv) to give **45** (35.0 mg, 70%) as a colorless oil: $R_f=0.15$ (EtOAc/*i*PrNH$_2$, 100:5); $[\alpha]_D^{20}=+4.4^\circ$ ($c=1.0$ in CH_2Cl_2); (^{1}H NMR 400 MHz, $CDCl_3$): $\delta=0.80$–0.89 (m, 1H), 0.90 (d, $J=6.6$ Hz, 6H), 0.99–1.10 (m, 1H), 1.15–1.29 (m, 2H), 1.36–1.45 (m, 2H), 1.49–1.70 (m, 9H), 1.70–1.78 (m, 2H), 1.79–1.92 (m, 2H), 2.02–2.14 (m, 3H), 2.14–2.23 (m, 1H), 2.24–2.30 (m, 2H), 2.30–2.39 (m, 2H), 2.64–2.75 (m, 2H), 2.84–2.94 (m, 2H), 3.16–3.29 (m, 3H), 3.31–3.40 (m, 1H), 3.44 (d, $J=13.2$ Hz, 1H), 3.50 (d, $J=13.2$ Hz, 1H), 3.98 (tt, $J=6.7$, 4.1 Hz, 1H), 4.86 (br s, 1H), 6.17 (t, $J=5.6$ Hz, 1H), 6.40 (br s, 1H), 7.20–7.26 (m, 1H), 7.28–7.33 ppm (m, 4H); ^{13}C NMR (100 MHz, $CDCl_3$): $\delta=22.7$, 22.7, 24.6, 25.1, 26.7, 26.8, 30.5, 30.9, 31.9, 33.5, 35.5, 35.7, 39.7, 39.9, 41.3, 44.7, 54.0, 54.2, 57.6, 59.2, 60.4, 63.3, 68.2, 126.9, 128.1, 129.0, 138.5, 171.8, 173.2 ppm; IR (film): $\tilde{\nu}=3293$, 2929, 2362, 1640, 1557, 1453, 1100, 734, 699 cm^{-1}; HRMS-ESI m/z $[M+Na]^+$ calcd for $C_{31}H_{52}N_4NaO_3^+$: 551.3932, found: 551.3933.

(*S*)-4-(2-((*R*)-1-Benzylpiperidin-3-yl)acetamido)-*N*-(3-((*R*)-1-isopentylpiperidin-3-yl)propyl)-2-methoxybutanamide (13). The reaction was performed according to general procedure 3 with acid **16a** (33.5 mg, 124 μmol, 1.19 equiv), and amine (derived from amide **43**, max. 104 μmol, 1.0 equiv) to give **13** (44.0 mg, 78%) as a colorless oil: $R_f=0.29$ (PE/EtOAc/*i*PrNH$_2$, 50:50:3); $[\alpha]_D^{20}=-13.7^\circ$ ($c=1.0$ in CH_2Cl_2); ^{1}H NMR (500 MHz, $CDCl_3$): $\delta=0.81$–0.89 (m, 1H), 0.90 (d, $J=6.6$ Hz, 6H), 0.97–1.06 (m, 1H), 1.15–1.28 (m, 2H), 1.38–1.45 (m, 2H), 1.50–1.69 (m, 9H), 1.71–1.84 (m, 3H), 1.84–1.91 (m, 3H), 1.99–2.05 (m, 2H), 2.06–2.15 (m, 2H), 2.30–2.38 (m, 2H), 2.64–2.70 (m, 1H), 2.73 (d, $J=10.0$ Hz, 1H), 2.85–2.94 (m, 2H), 3.17–3.32 (m, 3H), 3.36–3.42 (m, 1H), 3.38 (s, 3H), 3.44 (d, $J=13.3$ Hz, 1H), 3.49 (d, $J=13.3$ Hz, 1H), 3.63 (t, $J=5.8$ Hz, 1H), 5.98 (t, $J=5.4$ Hz, 1H), 6.62–6.68 (m, 1H), 7.21–7.26 (m, 1H), 7.28–7.32 ppm (m, 4H); ^{13}C NMR (125 MHz, $CDCl_3$): $\delta=22.7$, 22.7, 24.6, 25.2, 26.8, 27.0, 30.5, 30.9, 31.8, 32.0, 33.6, 35.6, 35.7, 35.9, 39.2, 41.6, 53.9, 54.2, 57.5, 58.3, 59.4, 60.4, 63.3, 80.9, 126.9, 128.1, 129.0, 138.6, 171.9, 171.9 ppm; IR (film): $\tilde{\nu}=3274$, 2931, 2362, 1648, 1541, 1456, 1115, 700 cm^{-1}; HRMS-ESI m/z $[M+Na]^+$ calcd for $C_{32}H_{54}N_4NaO_3^+$: 565.4088, found: 565.4086.

(*S*)-4-(2-((*R*)-1-Benzylpiperidin-3-yl)-*N*-methylacetamido)-*N*-(3-((*R*)-1-isopentylpiperidin-3-yl)propyl)-2-methoxybutanamide (46). The reaction was performed according to general procedure 3 with acid **16a** (35.9 mg, 133 μmol, 1.09 equiv), and crude amine (derived from amide **44**, max. 122 μmol, 1.0 equiv) to give **46** (58.7 mg, 86%) as a colorless oil: $R_f=0.40$ (PE/EtOAc/*i*PrNH$_2$, 50:50:3); $[\alpha]_D^{20}=-12.8^\circ$ ($c=1.0$ in CH_2Cl_2); ^{1}H NMR (500 MHz, $CDCl_3$): $\delta=0.78$–0.86 (m, 1H), 0.88 (d, $J=6.6$ Hz, 6H), 0.95–1.05 (m, 1H), 1.14–1.26 (m, 2H), 1.34–1.41 (m, 2H), 1.48–1.67 (m, 9H), 1.70–1.91 (m, 5H), 1.91–2.04 (m, 2H), 2.10–2.20 (m, 2H), 2.20–2.33 (m, 3H), 2.62–2.70 (m, 1H), 2.74–2.81 (m, 1H), 2.82–2.87 (m, 2H), 2.87 (s, 1.2H), 2.95 (s, 1.8H), 3.12–3.31 (m, 3H), 3.33–3.39 (m, 0.4H), 3.35 (s, 1.8H), 3.38 (s, 1.2H), 3.40–3.45 (m, 1H), 3.46–3.53 (m, 1H), 3.55 (dd, $J=7.0$, 4.4 Hz, 0.6H), 3.60 (dd, $J=7.1$, 4.1 Hz, 0.4H), 3.65–3.72 (m, 0.6H), 6.51 (t, $J=5.7$ Hz, 0.4H), 6.73 (t, $J=5.8$ Hz, 0.6H), 7.17–7.24 (m, 1H), 7.25–7.31 ppm (m, 4H), ^{13}C NMR (125 MHz, $CDCl_3$): $\delta=22.7$, 22.7, 24.8, 25.3, 26.8, 27.0, 27.0*, 29.9, 30.8*, 30.8, 31.0, 31.1*, 31.8*, 31.8, 33.0, 33.2*, 33.3*, 35.5, 35.8, 35.9, 37.3*, 38.0, 39.1, 39.1*, 43.6, 45.8*, 53.7*, 53.8, 54.2*, 54.3, 57.6, 58.1, 58.3*, 59.7, 59.8*, 60.6, 63.3*, 63.3, 79.9*, 80.0, 126.7, 128.0, 129.0, 138.6, 171.1*, 171.8*, 171.8, 171.9 ppm;[61b] IR (film): $\tilde{\nu}=3309$, 2929, 2362, 1646, 1532, 1456, 1111, 699 cm^{-1}; HRMS-ESI m/z $[M+H]^+$ calcd for $C_{33}H_{57}N_4O_3^+$: 557.4425, found: 557.4423.

General procedure 4: coupling of fragment 21a with middle fragments 17–20 to give amides 47–50. The Cbz-protected γ-amino acid (1.3–2.0 equiv) was dissolved in dry THF (0.1 M) at RT. Et_3N was added (5 equiv with respect to the amino acid) followed by DEPBT (2 equiv with respect to the amino acid) and the mixture was stirred at RT for 1–2 h. The resulting bright-green solution was cannulated to a mixture of the amine **21a** (1.0 equiv) and solid Na_2CO_3 (5 equiv with respect to **21a**) and the reaction mixture was stirred at RT overnight. Half-saturated $NaHCO_3$ solution was added, and after being stirred for 30 min it was extracted with EtOAc (five times). The combined organic extracts were dried ($MgSO_4$) and concentrated in vacuo. The crude product was purified by column chromatography (SiO_2, 3% $NEtMe_2$ in PE/EtOAc) followed by reversed-phase HPLC purification. (KNAUER Eurospher II 100 RP-C_{18}; 5 μm, 250×16 mm; eluent: MeCN/H_2O)

Benzyl ((2*R*,3*S*)-4-(((4*R*,5*R*,9*S*)-4,10-dimethoxy-5,9-dimethyl-6-oxodecyl)amino)-2-hydroxy-3-methyl-4-oxobutyl)(methyl)carbamate (47). The reaction was performed according to general procedure 4 with **17** (39.0 mg, 0.139 mmol, 1.6 equiv), and crude amine **21a** (25.5 mg, max. 86.7 μmol, 1.0 equiv) to give **47** (28.1 mg, 62% over two steps) as a colorless oil; $R_f=0.37$ (PE/EtOAc/NEtMe$_2$, 30:70:3); $[\alpha]_D^{20}=-14.3^\circ$ ($c=0.5$ in CH_2Cl_2); ^{1}H NMR (500 MHz, CD_2Cl_2): $\delta=0.88$ (d, $J=6.7$ Hz, 3H), 0.94 (d, $J=7.0$ Hz, 3H), 1.23 (d, $J=6.9$ Hz, 3H), 1.31–1.45 (m, 2H), 1.46–1.59 (m, 3H), 1.60–1.72 (m, 2H), 2.16–2.24 (m, 0.3H), 2.27–2.34 (m, 0.7H), 2.45 (ddd, $J=17.5$, 8.9, 6.3 Hz, 1H), 2.51 (ddd, $J=17.5$, 9.0, 6.3 Hz, 1H), 2.76 (virt. quint., $J=7.2$ Hz, 1H), 2.99 (s, 3H), 3.05–3.23 (m, 3H), 3.15 (dd, $J=9.2$, 6.1 Hz, 1H), 3.19 (dd, $J=9.2$, 6.1 Hz, 1H), 3.24 (s, 3H), 3.28 (s, 3H), 3.37–3.44 (m, 1.3H), 3.49 (dd, $J=14.2$, 5.6 Hz, 0.7H), 3.68–3.77 (m, 1H), 4.04 (br s, 1H), 5.11 (s, 2H), 5.92 (br s, 0.3H), 6.59 (br s, 0.7H), 7.28–7.34 (m, 1H), 7.35–7.40 ppm (m, 4H);^{13}C NMR (125 MHz, CD_2Cl_2): $\delta=12.5$*, 12.7, 16.2, 16.4*, 17.3, 24.9, 25.0*, 27.8, 27.8, 33.4, 36.2, 36.6*, 39.7*, 39.8, 40.9, 43.3, 43.5*, 49.4, 54.0*, 54.7, 57.8, 59.0, 67.5*, 67.7, 73.3, 73.5*, 78.7, 82.4*, 82.6, 128.2, 128.5, 129.0, 137.5, 157.9, 175.7, 176.0*, 213.8 ppm;[61f] HRMS-ESI m/z $[M+H]^+$ calcd for $C_{28}H_{47}N_2O_7^+$: 523.3378, found: 523.3379.

Benzyl ((*R*)-4-(((4*R*,5*R*,9*S*)-4,10-dimethoxy-5,9-dimethyl-6-oxodecyl)amino)-2-hydroxy-4-oxobutyl)carbamate (48). The reaction was performed according to general procedure 4 with **18** (57.8 mg, 0.228 mmol, 2.0 equiv), and crude amine **21a** (33.2 mg, max. 0.112 mmol, 1.0 equiv) to give **48** (34.3 mg, 62% over two steps) as a colorless oil: $R_f=0.22$ (EtOAc/NEtMe$_2$, 100:3); $[\alpha]_D^{20}=-17.7^\circ$ ($c=1.0$ in CH_2Cl_2); ^{1}H NMR (400 MHz, CD_2Cl_2): $\delta=0.88$ (d, $J=6.7$ Hz, 3H), 0.95 (d, $J=7.1$ Hz, 3H), 1.29–1.44 (m, 2H), 1.47–1.59 (m, 3H), 1.60–1.73 (m, 2H), 2.23–2.35 (m, 2H), 2.45 (ddd, $J=17.5$, 8.6, 5.9 Hz, 1H), 2.52 (ddd, $J=17.5$, 8.9, 6.3 Hz, 1H), 2.77 (quint., $J=7.1$ Hz, 1H), 3.15 (dd, $J=9.3$, 6.2 Hz, 1H), 3.17–3.24 (m, 3H), 3.19 (dd, $J=9.3$, 6.0 Hz, 1H), 3.25 (s, 3H), 3.28 (s, 3H), 3.29–3.35 (m, 1H), 3.38–3.43 (m, 1H), 4.02 (dddd, $J=7.9$, 6.5, 4.0, 3.9 Hz, 1H), 4.41 (br s, 1H), 5.08 (s, 2H), 5.42 (t, $J=6.1$ Hz, 1H), 6.18 (t, $J=6.1$ Hz, 1H), 7.28–7.33 (m, 1H), 7.33–7.37 ppm (m, 4H); ^{13}C NMR (100 MHz, CD_2Cl_2): $\delta=12.5$, 17.3, 25.0, 27.8, 27.8, 33.4, 39.9, 40.1, 40.8, 46.7,

49.3, 57.9, 59.0, 67.2, 68.6, 78.7, 82.5, 128.4, 128.6, 129.0, 137.4, 157.5, 172.4, 213.9 ppm; HRMS-ESI *m/z* $[M+Na]^+$ calcd for $C_{26}H_{42}N_2NaO_7^+$: 517.2884, found: 517.2886.

Benzyl ((*S*)-4-(((4*R*,5*R*,9*S*)-4,10-dimethoxy-5,9-dimethyl-6-oxodecyl)amino)-3-methoxy-4-oxobutyl)carbamate (49). The reaction was performed according to general procedure 4 with **19** (51.5 mg, 0.193 mmol, 1.5 equiv), and crude amine **21a** (37.5 mg, max. 0.127 mmol, 1.0 equiv) to give **49** (36.7 mg, 57% over two steps) as a colorless oil: $R_f=0.26$ (PE/EtOAc/NEtMe$_2$, 50:50:3); $[\alpha]_D^{20}=-33.9^\circ$ ($c=1.0$ in CH_2Cl_2); ^{1}H NMR (400 MHz, CD_2Cl_2): $\delta=0.88$ (d, $J=6.6$ Hz, 3H), 0.94 (d, $J=7.0$ Hz, 3H), 1.29–1.44 (m, 2H), 1.50–1.61 (m, 3H), 1.62–1.71 (m, 2H), 1.81–1.97 (m, 2H), 2.45 (ddd, $J=17.5$, 8.7, 5.9 Hz, 1H), 2.51 (ddd, $J=17.5$, 8.9, 6.3 Hz, 1H), 2.77 (dq, $J=7.8$, 7.0 Hz, 1H), 3.15 (dd, $J=9.3$, 6.2 Hz, 1H), 3.19 (dd, $J=9.3$, 6.0 Hz, 1H), 3.21–3.29 (m, 3H), 3.24 (s, 3H), 3.28 (s, 3H), 3.30–3.35 (m, 1H), 3.38 (s, 3H), 3.39–3.44 (m, 1H), 3.64 (dd, $J=6.7$, 5.0 Hz, 1H), 5.06 (s, 2H), 5.19–5.27 (m, 1H), 6.68 (t, $J=5.2$ Hz, 1H), 7.27–7.34 (m, 1H), 7.34–7.41 ppm (m, 4H); ^{13}C NMR (75 MHz, CD_2Cl_2): $\delta=12.6$, 17.3, 25.1, 27.7, 27.8, 33.1, 33.4, 38.2, 39.4, 40.9, 49.3, 57.8, 58.9, 59.0, 66.9, 78.7, 81.4, 82.5, 128.5, 128.4, 129.0, 137.7, 156.8, 172.2, 213.7 ppm; HRMS-ESI *m/z* $[M+Na]^+$ calcd for $C_{27}H_{44}N_2NaO_7^+$: 531.3041, found: 531.3040.

Benzyl ((*S*)-4-(((4*R*,5*R*,9*S*)-4,10-dimethoxy-5,9-dimethyl-6-oxodecyl)amino)-3-methoxy-4-oxobutyl)(methyl)carbamate (50). The reaction was performed according to general procedure 4 with **20** (48.6 mg, 0.178 mmol, 1.5 equiv), and amine **21a** (33.2 mg, max. 0.112 mmol, 1.0 equiv) to give **50** (35.7 mg, 61% over two steps) as a colorless oil: $R_f=0.30$ (PE/EtOAc/NEtMe$_2$, 50:50:3); $[\alpha]_D^{20}=-41.3^\circ$ ($c=1.0$ in CH_2Cl_2); ^{1}H NMR (400 MHz, CD_2Cl_2): $\delta=0.88$ (d, $J=6.7$ Hz, 3H), 0.94 (d, $J=7.0$ Hz, 3H), 1.31–1.44 (m, 2H), 1.49–1.60 (m, 3H), 1.60–1.72 (m, 2H), 1.75–1.88 (m, 1H), 1.99 (dddd, $J=14.0$, 8.5, 6.6, 4.2 Hz, 1H), 2.45 (ddd, $J=17.5$, 8.6, 5.9 Hz, 1H), 2.51 (ddd, $J=17.5$, 8.9, 6.2 Hz, 1H), 2.76 (virt. quint., $J=7.3$ Hz, 1H), 2.90 (s, 3H), 3.15 (dd, $J=9.1$, 6.0 Hz, 1H), 3.19 (dd, $J=9.1$, 6.0 Hz, 1H), 3.20–3.27 (m, 2H), 3.24 (s, 3H), 3.27–3.31 (m, 2H), 3.28 (s, 3H), 3.33–3.50 (m, 4H), 3.57 (dd, $J=7.6$, 4.2 Hz, 1H), 5.10 (s, 2H), 6.71 (br s, 0.5H), 6.59 (br s, 0.5H), 7.27–7.33 (m, 1H), 7.34–7.38 ppm (m, 4H); ^{13}C NMR (100 MHz, CD_2Cl_2): $\delta=12.6$, 17.3, 25.1, 27.8, 27.8, 31.1, 31.4*, 33.4, 34.4, 35.0*, 39.4, 40.9, 45.5, 45.9*, 49.3, 57.8, 58.7, 58.8*, 59.0, 67.3, 78.7, 80.9, 82.6, 128.2, 128.4, 128.9, 137.9, 156.5, 156.7*, 172.0, 172.2*, 213.7 ppm;[61a] HRMS-ESI *m/z* $[M+Na]^+$ calcd for $C_{28}H_{46}N_2NaO_7^+$: 545.3197, found: 545.3197.

General procedure 5: Cbz deprotection of amides 47–50. Pd/C (10%, 2.0 mg per 1.0 mg amide) was added to a stirred solution of Cbz protected amide **47–50** in 0.075 M methanolic HCl (7.0 mg mL^{-1}). The resulting reaction mixture was stirred for 25 min under an atmosphere of H_2. Afterward, the reaction mixture was filtered through a PTFE syringe filter (Chromafil Xtra, PTFE-45/25 0.45 μm). The resulting filtrate was concentrated in vacuo to yield the crude amines (91–95%) as hydrochlorides which were used directly without further purification.

(2*S*,3*R*)-4-(2-((*R*)-1-Benzylpiperidin-3-yl)-*N*-methylacetamido)-*N*-((4*R*,5*R*,9*S*)-4,10-dimethoxy-5,9-dimethyl-6-oxodecyl)-3-hydroxy-2-methylbutanamide (14). The reaction was performed according to general procedure 3 with **16a** (18.6 mg, 68.9 μmol, 2.1 equiv), and crude amine (derived from amide **47**, max. 32.2 μmol, 1.0 equiv) to give **14** (14.7 mg, 76% over two steps) as a colorless oil: $R_f=0.13$ (PE/EtOAc/NEtMe$_2$, 25:75:3); $[\alpha]_D^{20}=-9.8^\circ$ ($c=0.5$ in CH_2Cl_2); ^{1}H NMR (500 MHz, CD_2Cl_2): $\delta=0.88$ (d, $J=6.7$ Hz, 3H), 0.94 (d, $J=7.0$ Hz, 2.7H), 0.96 (d, $J=7.3$ Hz, 0.3H), 0.97–1.08 (m, 1H), 1.20 (d, $J=7.1$ Hz, 2.7H), 1.27 (d, $J=7.1$ Hz, 0.3H), 1.29–1.36 (m, 1H), 1.36–1.46 (m, 1H), 1.49–1.59 (m, 4H), 1.59–1.71 (m, 3H), 1.72–1.83 (m, 2H), 1.94–2.02 (m, 1H), 2.04–2.14 (m, 1H), 2.16–2.22 (m, 1H), 2.22–2.30 (m, 2H), 2.45 (ddd, $J=17.5$, 8.9, 5.8 Hz, 1H), 2.51 (ddd, $J=17.5$, 9.1, 6.2 Hz, 1H), 2.62–2.70 (m, 1H), 2.72–2.80 (m, 2H), 2.88 (s, 0.3H), 3.03 (s, 2.7H), 3.12–3.19 (m, 2H), 3.19–3.23 (m, 3H), 3.24 (s, 2.7H), 3.25 (s, 0.3H), 3.28 (s, 3H), 3.35–3.52 (m, 3H), 3.57 (dd, $J=13.9$, 5.2 Hz, 1H), 3.61–3.67 (m, 0.9H), 3.73–3.78 (m, 0.1H), 4.40 (d, $J=5.6$ Hz, 1H), 6.17 (t, 6.0 Hz, 0.1H), 6.75 (t, $J=5.3$ Hz, 0.9H), 7.19–7.26 (m, 1H), 7.26–7.34 ppm (m, 4H); ^{13}C NMR (125 MHz, CD_2Cl_2): $\delta=12.5$*, 12.8, 16.0, 16.2*, 17.3, 24.9, 25.1*, 25.5, 27.7, 27.8, 31.4, 33.4, 33.6, 34.5*, 37.9, 38.4, 39.8, 40.8*, 41.0, 43.9*, 44.1, 49.2*, 49.4, 54.3, 54.5, 54.8*, 57.8, 59.0, 60.4, 63.9, 72.5*, 73.6, 78.6, 82.4*, 82.6, 127.3, 128.6, 129.5, 139.6, 174.3, 175.4, 213.8 ppm;[61e] IR (film): $\tilde{\nu}=3309$, 2931, 2361, 1711, 1646, 1558, 1456, 1100, 700 cm^{-1}; HRMS-ESI *m/z* $[M+H]^+$ calcd for $C_{34}H_{57}N_3O_6^+$: 604.4320, found: 604.4324.

(*R*)-4-(2-((*R*)-1-Benzylpiperidin-3-yl)acetamido)-*N*-((4*R*,5*R*,9*S*)-4,10-dimethoxy-5,9-dimethyl-6-oxodecyl)-3-hydroxybutanamide (51). The reaction was performed according to general procedure 3 with **16a** (14.8 mg, 54.9 μmol, 2.1 equiv), and crude amine (derived from amide **48**, max. 26.5 μmol, 1.0 equiv) to give **51** (10.6 mg, 70% over two steps) as a colorless oil: $R_f=0.19$ (EtOAc/NEtMe$_2$, 100:6); $[\alpha]_D^{20}=-14.7^\circ$ ($c=0.5$ in CH_2Cl_2); ^{1}H NMR (500 MHz, CD_2Cl_2): $\delta=0.88$ (d, $J=6.7$ Hz, 3H), 0.94 (d, $J=7.0$ Hz, 3H), 0.97–1.07 (m, 1H), 1.30–1.45 (m, 2H), 1.48–1.59 (m, 4H), 1.59–1.69 (m, 3H), 1.69–1.75 (m, 1H), 1.79 (t, $J=9.9$ Hz, 1H), 1.96–2.09 (m, 3H), 2.09–2.18 (m, 1H), 2.18–2.29 (m, 2H), 2.46 (ddd, $J=17.5$, 8.8, 5.7 Hz, 1H), 2.51 (ddd, $J=17.5$, 9.0, 6.2 Hz, 1H), 2.61–2.69 (m, 1H), 2.63–2.68 (m, 1H), 2.73–2.80 (m, 1H), 3.12–3.24 (m, 5H), 3.24 (s, 3H), 3.28 (s, 3H), 3.34 (ddd, $J=13.9$, 6.3, 3.6 Hz, 1H), 3.38–3.43 (m, 1H), 3.41 (d, $J=13.1$ Hz, 1H), 3.47 (d, $J=13.1$ Hz, 1H), 3.94 (ddt, $J=7.9$, 6.3, 4.0 Hz, 1H), 4.66 (br s, 1H), 6.11 (t, $J=5.5$ Hz, 1H), 6.34 (t, $J=5.3$ Hz, 1H), 7.20–7.25 (m, 1H), 7.27–7.31 ppm (m, 4H); ^{13}C NMR (125 MHz, CD_2Cl_2): $\delta=12.6$, 17.3, 25.0, 25.4, 27.8, 27.8, 31.1, 33.4, 34.2, 39.9, 40.4, 40.9, 41.7, 45.3, 49.3, 54.6, 57.9, 59.0, 60.0, 63.8, 68.8, 78.7, 82.5, 127.4, 128.6, 129.5, 139.6, 172.3, 173.5, 213.8 ppm; IR (film): $\tilde{\nu}=3295$, 2931, 2360, 1711, 1646, 1542, 1456, 1100, 700 cm^{-1}; HRMS-ESI *m/z* $[M+H]^+$ calcd for $C_{32}H_{54}N_3O_6^+$: 576.4007, found: 576.4005.

(*S*)-4-(2-((*R*)-1-Benzylpiperidin-3-yl)acetamido)-*N*-((4*R*,5*R*,9*S*)-4,10-dimethoxy-5,9-dimethyl-6-oxodecyl)-2-methoxybutanamide (15). The reaction was performed according to general procedure 3 with **16a** (18.6 mg, 68.9 μmol, 2.1 equiv), and crude amine (derived from amide **49**, max. 32.2 μmol, 1.0 equiv) to give **15** (14.7 mg, 77% over two steps) as a colorless oil: $R_f=0.18$ (PE/EtOAc/NEtMe$_2$, 40:60:3); $[\alpha]_D^{20}=-30.8^\circ$ ($c=0.5$ in CH_2Cl_2); ^{1}H NMR (500 MHz, CD_2Cl_2): $\delta=0.88$ (d, $J=6.7$ Hz, 3H), 0.94 (d, $J=7.1$ Hz, 3H), 0.97–1.04 (m, 1H), 1.30–1.43 (m, 2H), 1.50–1.58 (m, 3H), 1.58–1.67 (m, 3H), 1.68–1.87 (m, 5H), 1.95–2.08 (m, 4H), 2.45 (ddd, $J=17.5$, 9.0, 6.1 Hz, 1H), 2.51 (ddd, $J=17.5$, 9.0, 6.2 Hz, 1H), 2.63–2.69 (m, 1H), 2.69–2.74 (m, 1H), 2.77 (dq, $J=7.8$, 7.1 Hz, 1H), 3.15 (dd, $J=9.2$, 6.1 Hz, 1H), 3.18–3.24 (m, 2H), 3.19 (dd, $J=9.2$, 6.1 Hz, 1H), 3.24 (s, 3H), 3.25–3.35 (m, 2H), 3.28 (s, 3H), 3.37 (s, 3H), 3.38–3.43 (m, 1H), 3.40 (d, $J=13.2$ Hz, 1H), 3.46 (d, $J=13.2$ Hz, 1H), 3.59 (dd, $J=6.5$, 5.3 Hz, 1H), 5.95 (t, $J=4.8$ Hz, 1H), 6.72 (t, $J=5.4$ Hz, 1H), 7.20–7.25 (m, 1H), 7.27–7.32 ppm (m, 4H); ^{13}C NMR (125 MHz, CD_2Cl_2): $\delta=$ 12.6, 17.3, 25.1, 25.5, 27.7, 27.8, 31.2, 32.8, 33.4, 34.2, 36.4, 39.4, 40.9, 42.0, 49.3, 54.5, 57.8, 58.8, 59.0, 60.1, 63.9, 78.6, 81.5, 82.5, 127.3, 128.6, 129.5, 139.7, 172.1, 172.3, 213.7 ppm; IR (film): $\tilde{\nu}=$ 3296, 2930, 2361, 1711, 1648, 1539, 1452, 1104, 699 cm^{-1}; HRMS-ESI *m/z* $[M+Na]^+$ calcd for $C_{33}H_{55}N_3NaO_6^+$: 612.3983, found: 612.3982.

(*S*)-4-(2-((*R*)-1-Benzylpiperidin-3-yl)-*N*-methylacetamido)-*N*-((4*R*,5*R*,9*S*)-4,10-dimethoxy-5,9-dimethyl-6-oxodecyl)-2-methoxybutanamide (52). The reaction was performed according to general procedure 3 with **16a** (15.3 mg, 56.7 μmol, 1.8 equiv), and crude amine (derived from amide **50**, max. 31.4 μmol, 1.0 equiv) to give **52** (14.8 mg, 78% over two steps) as a colorless oil: $R_f = 0.19$ (PE/EtOAc/NEtMe$_2$, 60:40:3); $[\alpha]_D^{20} = -32.7^\circ$ ($c = 0.5$ in CH_2Cl_2); ^{1}H NMR (500 MHz, CD_2Cl_2): $\delta = 0.88$ (d, $J = 6.6$ Hz, 3H), 0.94 (d, $J = 7.1$ Hz, 1.8H), 0.95 (d, $J = 7.1$ Hz, 1.2H), 0.98–1.05 (m, 1H), 1.30–1.43 (m, 2H), 1.50–1.70 (m, 7H), 1.70–1.80 (m, 2H), 1.81–2.02 (m, 3H), 2.04–2.11 (m, 1H), 2.11–2.27 (m, 2H), 2.42–2.54 (m, 2H), 2.62–2.70 (m, 1H), 2.73–2.80 (m, 2H), 2.83 (s, 1.2H), 2.94 (s, 1.8H), 3.13–3.21 (m, 2H), 3.21–3.30 (m, 2H), 3.24 (s, 1.8H), 3.25 (s, 1.2H), 3.28 (s, 3H), 3.34 (s, 1.8H), 3.34–3.43 (m, 3H), 3.38 (s, 1.2H), 3.45–3.59 (m, 3H), 6.63 (t, $J = 5.8$ Hz, 0.4H), 6.78 (t, $J = 5.6$ Hz, 0.6H), 7.19–7.25 (m, 1H), 7.26–7.32 ppm (m, 4H); ^{13}C NMR (125 MHz, CD_2Cl_2): $\delta = 12.4$*, 12.5, 17.1, 24.9, 25.0*, 25.4, 27.6 (2C), 30.7, 31.3*, 31.4, 31.6*, 33.2, 33.3*, 33.5*, 33.7, 35.8, 37.7*, 38.3, 39.2, 39.3*, 40.7*, 40.8, 44.2, 46.2*, 49.1*, 49.2, 54.3, 54.3*, 57.7, 57.7*, 58.6, 58.7*, 58.8, 60.3, 60.4*, 63.7, 78.5, 80.4*, 80.8, 82.3*, 82.4, 127.1, 128.4, 129.3, 139.5, 171.5, 171.8*, 172.0*, 172.1, 213.4*, 213.5 ppm;[61b] IR (film): $\tilde{\nu} = 3310$, 2930, 2363, 1712, 1646, 1526, 1405, 1106, 700 cm^{-1}; HRMS-ESI *m/z* $[M+H]^+$ calcd for $C_{34}H_{57}N_3O_6^+$: 604.4320, found: 604.4323.

Biological evaluations

Cell culture and growth inhibition assays. Mammalian cervical carcinoma cell line KB-31 and human mammary carcinoma cell line MCF-7 were obtained from the German collection of Microorganisms and Cell Cultures (DSMZ). Growth inhibition was measured as previously described, and metabolic activity was determined after five days by 3-(4,5-dimethylthiazol-2-yl)-2,5-diphenyltetrazolium bromide (MTT) assay.[53]

Fluorescence microscopy. Potoroo (*Potorous tridactylis*) PtK_2 (NCL-5) kidney cells (ATCC CCL 56) from the German collection of Microorganisms and Cell Cultures (DSMZ) were grown on ME medium supplemented with nonessential amino acids and 10% fetal bovine serum. Growth conditions and details on the fluorescence microscopy studies were described previously.[17b] The novel ligands were evaluated at concentrations of 25 μg mL^{-1}.

Acknowledgements

We thank the Deutsche Forschungsgemeinschaft (DFG; Me 2756/4-1 and Forschergruppe 1406) and the DFG Graduiertenkolleg 850 (scholarship to S.D.) for generous funding, Julian Horn and Raiko Hahn for technical assistance, and Andreas Schneider for excellent assistance with HPLC separations.

Keywords: actin · analogues · bistramide · polyketides · rhizopodin

[1] T. D. Pollard, L. Blanchoin, R. D. Mullins, *Annu. Rev. Biophys. Biomol. Struct.* **2000**, *29*, 545–576.
[2] T. P. Stossel, *J. Biol. Chem.* **1989**, *264*, 18261–18264.
[3] M. A. Jordan, L. Wilson, *Curr. Opin. Cell Biol.* **1998**, *10*, 123–130.
[4] A. Giganti, E. Friederich, *Prog. Cell Cycle Res.* **2003**, *5*, 511–525.
[5] a) L. A. Cameron, P. A. Giardini, F. S. Soo, J. A. Theriot, *Nat. Rev. Mol. Cell Biol.* **2000**, *1*, 110–119; b) A. Ploubidou, M. Way, *Curr. Opin. Cell Biol.* **2001**, *13*, 97–105.
[6] I. Spector, F. Braet, N. R. Shochet, M. Bubb, *Microsc. Res. Tech.* **1999**, *47*, 18–37.
[7] L. R. Otterbein, P. Graceffa, R. Dominguez, *Science* **2001**, *293*, 708–711.
[8] For reviews, see: a) K.-S. Yeung, I. Paterson, *Angew. Chem. Int. Ed.* **2002**, *41*, 4632–4653; *Angew. Chem.* **2002**, *114*, 4826–4847; b) J. S. Allingham, V. A. Klenchin, I. Rayment, *Cell. Mol. Life Sci.* **2006**, *63*, 2119–2134.
[9] Other natural products, such as the latrunculins, selectively address the ATP binding pocket between domains 2 and 4, leading to significant conformational changes within both these domains. As a result, the actin monomers can no longer interact with the existing filament or other monomers, and therefore, polymerization is effectively suppressed: a) I. Spector, N. R. Shochet, Y. Kashman, A. Groweiss, *Science* **1983**, *219*, 493–495; b) M. Coué, S. L. Brenner, I. Spector, E. D. Korn, *FEBS Lett.* **1987**, *213*, 316–318.
[10] a) J. Tanaka, Y. Yan, J. Choi, J. Bai, V. A. Klenchin, I. Rayment, G. Marriott, *Proc. Natl. Acad. Sci. USA* **2003**, *100*, 13851–13856; b) V. A. Klenchin, J. Allingham, R. King, J. Tanaka, G. Marriott, I. Rayment, *Nat. Struct. Mol. Biol.* **2003**, *10*, 1058–1063.
[11] a) J. A. Roesener, P. J. Scheuer, *J. Am. Chem. Soc.* **1986**, *108*, 846–847; b) S. Matsunaga, N. Fusetani, K. Hashimoto, *J. Am. Chem. Soc.* **1986**, *108*, 847–849; c) M. R. Kernan, T. F. Molinski, D. J. Faulkner, *J. Org. Chem.* **1988**, *53*, 5014–5020; d) S. Matsunaga, N. Fusetani, K. Hashimoto, K. Koseki, M. Noma, H. Noguchi, U. Sankawa, *J. Org. Chem.* **1989**, *54*, 1360–1363.
[12] a) G. Guella, I. Mancini, G. Chiasera, F. Pietra, *Helv. Chim. Acta* **1989**, *72*, 237–246; b) M. V. D'Auria, L. Gomez-Paloma, L. Minale, A. Zampella, J. F. Verbist, C. Roussakis, C. Debitus, *Tetrahedron* **1993**, *49*, 8657–8664; c) M. V. D'Auria, L. Gomez-Paloma, L. Minale, A. Zampella, J. F. Verbist, C. Roussakis, C. Debitus, J. Patissou, *Tetrahedron* **1994**, *50*, 4829–4834; d) C. Bassarello, G. Bifulco, A. Zampella, M. V. D'Auria, R. Riccio, L. Gomez-Paloma, *Eur. J. Org. Chem.* **2001**, 39–44; e) J. S. Allingham, A. Zampella, M. V. D'Auria, I. Rayment, *Proc. Natl. Acad. Sci. USA* **2005**, *102*, 14527–14532; f) R. D. Perrins, G. Cecere, I. Paterson, G. Marriott, *Chem. Biol.* **2008**, *15*, 287–294.
[13] a) S. Carmely, Y. Kashman, *Tetrahedron Lett.* **1985**, *26*, 511–514; b) Y. Kato, N. Fusetani, S. Matsunaga, K. Hashimoto, R. Sakai, T. Higa, Y. Kashman, *Tetrahedron Lett.* **1987**, *28*, 6225–6228; c) M. Kobayashi, J. Tanaka, T. Katori, M. Matsuura, M. Yamashita, I. Kitagawa, *Chem. Pharm. Bull.* **1990**, *38*, 2409–2418; d) M. Doi, T. Ishida, M. Kobayashi, I. Kitagawa, *J. Org. Chem.* **1991**, *56*, 3629–3632; e) S. Tsukamoto, M. Ishibashi, T. Sasaki, J. Kobayashi, *J. Chem. Soc. Perkin Trans. 1* **1991**, 3185–3188; f) J. S. Todd, K. A. Alvi, P. Crews, *Tetrahedron Lett.* **1992**, *33*, 441–442; g) M. Kobayashi, K. Kawazoe, T. Okamoto, T. Sasaki, I. Kitagawa, *Chem. Pharm. Bull.* **1994**, *42*, 19–26.
[14] a) K. Yamada, M. Ojika, T. Ishigaki, Y. Yoshida, H. Ekimoto, M. Arakawa, *J. Am. Chem. Soc.* **1993**, *115*, 11020–11021; b) M. Ojika, H. Kigoshi, T. Ishigaki, T. Tsuboi, T. Ogawa, K. Yamada, *J. Am. Chem. Soc.* **1994**, *116*, 7441–7442.
[15] a) D. Gouiffès, S. Moreau, N. Helbecque, J. L. Bernier, J. P. Hénichart, Y. Barbin, D. Laurent, J. F. Verbist, *Tetrahedron* **1988**, *44*, 451–459; b) C. Roussakis, N. Robillard, D. Riou, J. F. Biard, G. Pradal, P. Piloquet, C. Debitus, J. F. Verbist, *Cancer Chemother. Pharmacol.* **1991**, *28*, 283–292; c) J. F. Biard, C. Roussakis, J. M. Kornprobst, D. Gouffes-Barbin, J. F. Verbist, *J. Nat. Prod.* **1994**, *57*, 1336–1345; d) D. Riou, C. Roussakis, J. F. Biard, J. F. Verbist, *Anticancer Res.* **1993**, *13*, 2331–2334; e) A. V. Statsuk, R. Bai, J. L. Baryza, V. A. Verma, E. Hamel, P. A. Wender, S. A. Kozmin, *Nat. Chem. Biol.* **2005**, *1*, 383–388; f) S. A. Rizvi, V. Tereshko, A. A. Kossiakoff, S. A. Kozmin, *J. Am. Chem. Soc.* **2006**, *128*, 3882–3883.
[16] J. C. Blain, Y.-F. Mok, J. Kubanek, J. S. Allingham, *Chem. Biol.* **2010**, *17*, 802–807.
[17] a) F. Sasse, H. Steinmetz, G. Höfle, H. Reichenbach, *J. Antibiot.* **1993**, *46*, 741–748; b) T. M. A. Gronewold, F. Sasse, H. Lünsdorf, H. Reichenbach, *Cell Tissue Res.* **1999**, *295*, 121–129; c) N. Horstmann, D. Menche, *Chem. Commun.* **2008**, 5173–5175; d) N. Oku, A. Matsumoto, T. Matsunaga, Y. Asano, H. Kasai, S. Matoba, Y. Igarashi, *Chem. Pharm. Bull.* **2014**, *62*, 294–300.
[18] For a review, see Ref. [10b].
[19] Rhizopodin: G. Hagelueken, G. Albrecht, R. Jansen, H. Steinmetz, D. Heinz, M. Kalesse, F. Sasse, W.-D. Schubert, *Angew. Chem. Int. Ed.* **2009**, *48*, 595–598; *Angew. Chem.* **2009**, *121*, 603–606.

[20] For a leading review on the total synthesis of actin binding macrolides, see Ref. [8].
[21] Total syntheses of bistramides: a) P. Wipf, T. D. Hopkins, *Chem. Commun.* **2005**, 3421 – 3423; b) M. T. Crimmins, A. C. DeBaillie, *J. Am. Chem. Soc.* **2006**, *128*, 4936 – 4937; c) J. T. Lowe, I. E. Wrona, J. S. Panek, *Org. Lett.* **2007**, *9*, 327 – 330; d) J. S. Yadav, L. Chetia, *Org. Lett.* **2007**, *9*, 4587 – 4589; e) L. Tomas, G. B. Gennas, M. A. Hiebel, P. Hampson, D. Gueyrard, B. Pelotier, J. Yli-Kauhaluoma, O. Piva, J. M. Lord, P. G. Goekjian, *Chem. Eur. J.* **2012**, *18*, 7452 – 7466.
[22] Total syntheses of rhizopodin: a) M. Dieckmann, M. Kretschmer, P. Li, S. Rudolph, D. Herkommer, D. Menche, *Angew. Chem. Int. Ed.* **2012**, *51*, 5667 – 5670; *Angew. Chem.* **2012**, *124*, 5765 – 5768; b) S. M. Dalby, J. M. Goodwin-Tindall, I. Paterson, *Angew. Chem. Int. Ed.* **2013**, *52*, 6517 – 6521; *Angew. Chem.* **2013**, *125*, 6645 – 6649; c) M. Kretschmer, M. Dieckmann, P. Li, S. Rudolph, D. Herkommer, J. Troendlin, D. Menche, *Chem. Eur. J.* **2013**, *19*, 15993 – 16018; formal total synthesis: d) K. K. Pulukuri, T. K. Chakraborty, *Org. Lett.* **2014**, *16*, 2284 – 2287.
[23] For synthetic studies toward rhizopodin, see: a) Z. Cheng, L. Song, Z. Xu, T. Ye, *Org. Lett.* **2010**, *12*, 2036 – 2039; b) T. Chakraborty, K. K. Pulukuri, M. Sreekanth, *Tetrahedron Lett.* **2010**, *51*, 6444 – 6446; c) T. K. Chakraborty, M. Sreekanth, K. K. Pulukuri, *Tetrahedron Lett.* **2011**, *52*, 59 – 61; d) K. K. Pulukuri, T. K. Chakraborty, *Org. Lett.* **2012**, *14*, 2858 – 2861; e) M. Kretschmer, D. Menche, *Org. Lett.* **2012**, *14*, 382 – 385; f) M. Dieckmann, S. Rudolph, S. Dreisigacker, D. Menche, *J. Org. Chem.* **2012**, *77*, 10782 – 10788; g) M. Dieckmann, S. Rudolph, C. Lang, W. Ahlbrecht, D. Menche, *Synthesis* **2013**, *45*, 2305 – 2315; h) M. Dieckmann, D. Menche, *Org. Lett.* **2013**, *15*, 228 – 231; i) T. Bender, D. Loits, J. M. White, M. A. Rizzacasa, *Org. Lett.* **2014**, *16*, 1450 – 1453.
[24] For a previous SAR study of a monomeric rhizopodin analogue, see: K. C. Nicolaou, X. Jiang, P. J. Lindsay-Scott, A. Corbu, S. Yamashiro, A. Bacconi, V. M. Fowler, *Angew. Chem. Int. Ed.* **2011**, *50*, 1139 – 1144; *Angew. Chem.* **2011**, *123*, 1171 – 1176.
[25] For previous SAR studies of bistramide analogues, see: I. E. Wrona, J. T. Lowe, T. J. Turbyville, T. R. Johnson, J. Beignet, J. A. Beutler, J. S. Panek, *J. Org. Chem.* **2009**, *74*, 1897 – 1916.
[26] During preparation of this manuscript, Marriott and co-workers reported the evaluation of side chain analogues based on these vinylamide side chains: J. H. Pereira, C. Petchprayoon, A. C. Hoepker, N. Moriarty, S. J. Fink, G. Cecere, I. Paterson, P. D. Adams, G. Marriott, *ChemMedChem* **2014**, *9*, 2286 – 2293.
[27] H. Kigoshi, K. Suenaga, M. Takagi, A. Akao, K. Kanematsu, N. Kamei, Y. Okugawa, K. Yamada, *Tetrahedron* **2002**, *58*, 1075 – 1102.
[28] A detailed analysis of the X-ray-derived binding interactions of aplyronine with actin has been reported: K. Hirata, S. Muraoka, K. Suenaga, T. Kuroda, K. Kato, H. Tanaka, M. Yamamoto, M. Takata, K. Yamada, H. Kigoshi, *J. Mol. Biol.* **2006**, *356*, 945 – 954.
[29] All figures represent the actin protein from the co-crystal with reidispongiolide A (PDB ID: 2ASM). Gelsolin was aligned from the corresponding co-crystal with actin (PDB ID: 1H1V). The position of bistramide in panels a) and b) was obtained by alignment from co-crystal PDB ID: 1FXU, and the position of kabiramide C was obtained by alignment from structure PDB ID: 1QZ5.
[30] G. M. Morris, D. S. Goodsell, R. S. Halliday, R. Huey, W. E. Hart, R. K. Belew, A. J. Olson, *J. Comput. Chem.* **1998**, *19*, 1639 – 1662.
[31] H. Gohlke, M. Hendlich, G. Klebe, *J. Mol. Biol.* **2000**, *295*, 337 – 356.
[32] The results for the smaller search areas (75 and 60 grid points in each dimension) are depicted in the Supporting Information. The docking convergence (number of structures in the highest populated cluster) are also summarized there.
[33] Residue F375 is located at the end of the protein sequence and not resolved in all crystal structures.
[34] a) Y.-G. Zhu, H.-Z. Kan, L.-Q. Jiang, W.-H. Hu, *Synth. Commun.* **2012**, *42*, 1137 – 1145; b) Enantiomeric excess was determined by HPLC analysis of a corresponding urea derivative according to: L. Merritt, J. S. Ward (Eli Lilly Co.), Int. PCT Pub. No. WO1998054179, **1998**; *Chem. Abstr.* **1998**, *130*, 38385; absolute configuration was confirmed by X-ray crystallography.
[35] P. Abraham, J. B. Pitner, A. H. Lewin, J. W. Boja, M. J. Kuhar, F. I. Carrol, *J. Med. Chem.* **1992**, *35*, 141 – 144.
[36] V. K. Yadav, K. G. Babu, *J. Org. Chem.* **2004**, *69*, 577 – 580.
[37] L. A. Marcaurelle, E. Comer, S. Dandapani, J. R. Duvall, B. Gerard, S. Kesavan, M. D. Lee IV, H. Liu, J. T. Lowe, J. Marie, C. A. Mulrooney, B. A. Pandya, A. Rowley, T. D. Ryba, B.-C. Suh, J. Wei, D. W. Young, L. B. Akella, N. T. Ross, Y.-L. Zhang, D. M. Fass, S. A. Reis, W.-N. Zhao, S. J. Haggarty, M. Palmer, M. A. Foley, *J. Am. Chem. Soc.* **2010**, *132*, 16962 – 16976.
[38] S. Nishiguchi, M. O. Sydnes, A. Taguchi, T. Regnier, T. Kajimoto, M. Node, Y. Yamazaki, F. Yakushiji, Y. Kiso, Y. Hayashi, *Tetrahedron* **2010**, *66*, 314 – 320.
[39] Y. Kobayashi, T. Tsuchiya, S. Umezawa, T. Yoneta, S. Fukatsu, H. Umezawa, *Bull. Chem. Soc. Jpn.* **1987**, *60*, 713 – 720.
[40] For a comprehensive review, see: J. Li, D. Menche, *Synthesis* **2009**, 2293 – 2315.
[41] a) A. Abiko, J.-F. Liu, S. Masamune, *J. Am. Chem. Soc.* **1997**, *119*, 2586 – 2587; b) T. Inoue, J.-F. Liu, D. C. Buske, A. Abiko, *J. Org. Chem.* **2002**, *67*, 5250 – 5256; c) A. Abiko, J.-F. Liu, *J. Org. Chem.* **1996**, *61*, 2590 – 2591.
[42] J. Li, P. Li, D. Menche, *Synlett* **2009**, 2417 – 2420.
[43] M. G. Organ, J. Wang, *J. Org. Chem.* **2003**, *68*, 5568 – 5574.
[44] B. Lal, B. N. Pramanik, M. S. Manhas, A. K. Bose, *Tetrahedron Lett.* **1977**, *18*, 1977 – 1980.
[45] a) O. Mitsunobu, *Synthesis* **1981**, 1 – 28; b) K. C. Kumara Swamy, N. N. Bhuvan Kumar, E. Balaraman, K. V. P. Pavan Kumar, *Chem. Rev.* **2009**, *109*, 2551 – 2651.
[46] Y. G. Gololobov, I. N. Zhmurova, L. F. Kasukhin, *Tetrahedron* **1981**, *37*, 437 – 472.
[47] W. Lin, X. Zhang, Z. He, Y. Jin, L. Gong, A. Mi, *Synth. Commun.* **2002**, *32*, 3279 – 3284.
[48] D. Enders, C. Thiebes, *Synthesis* **2000**, 510 – 512.
[49] H. Li, X. Jiang, Y. Ye, C. Fan, T. Romoff, M. Goodman, *Org. Lett.* **1999**, *1*, 91 – 93.
[50] J. D. More, N. S. Finney, *Org. Lett.* **2002**, *4*, 3001 – 3003.
[51] W. S. Wadsworth, W. D. Emmons, *J. Am. Chem. Soc.* **1961**, *83*, 1733 – 1738.
[52] a) T. Yasuhara, K. Nishimura, M. Yamashita, N. Fukuyama, K.-I. Yamada, O. Muraoka, K. Tomioka, *Org. Lett.* **2003**, *5*, 1123 – 1126; b) M. E. Kuehne, S. D. Cowen, F. Xu, L. S. Borman, *J. Org. Chem.* **2001**, *66*, 5303 – 5316.
[53] a) M. Ishiyama, H. Tominaga, M. Shiga, K. Sasamoto, Y. Ohkura, K. Ueno, *Biol. Pharm. Bull.* **1996**, *19*, 1518 – 1520; b) F. Sasse, H. Steinmetz, T. Schupp, F. Petersen, K. Memmert, H. Hofmann, C. Heusser, V. Brinkmann, P. Von Matt, G. Höfle, H. Reichenbach, *J. Antibiot.* **2002**, *55*, 543 – 551.
[54] Exemplarily data for comparison, Ref. [17]: chronic myelogenous leukemia cell line K-562: 15 ng mL^{-1}; BHK (GBF, hamster): 30 ng mL^{-1}; L929 (mouse): 15 ng mL^{-1}.
[55] Compound **53** was prepared by coupling a diastereomeric mixture of **21 a** (derived from reaction of **34** with an older, partially racemized batch of Roche aldehyde **35**) with 1.5 equiv (2*S*,3*R*)-4-((*tert*-butoxycarbonyl)(methyl)amino)-3-hydroxy-2-methylbutanoic acid (see synthesis of **17**) using DEPBT (3.0 equiv), Et_3N (7.5 equiv), and Na_2CO_3 (5.0 equiv) in 51% yield.
[56] Compound **54** was prepared by coupling a diastereomeric mixture of **21 a** (derived from reaction of **34** with an older, partially racemized batch of Roche aldehyde **35**) with **19** (1.4 equiv) using DEPBT (3.0 equiv), Et_3N (7.5 equiv), and Na_2CO_3 (5.0 equiv) in 68% yield.
[57] In agreement with these data, very little or no effects on the actin polymerization were visible in in vitro assays (actin polymerization biochem kit muscle actin, with rhizopodin as control) at concentrations up to 1000 μM; see the Supporting Information for details.
[58] Macromodel ver. 9.7, Schrödinger LLC, New York, NY (USA), **2009**.
[59] W. L. Jorgensen, D. S. Maxwell, J. Tirado-Rivers, *J. Am. Chem. Soc.* **1996**, *118*, 11225 – 11236.
[60] C. A. Sotriffer, H. Gohlke, G. Klebe, *J. Med. Chem.* **2002**, *45*, 1967 – 1970.
[61] Extra signals due to amide conformers marked with an asterisk: a) conformer ratio = 1:1; b) conformer ratio = 6:4; c) conformer ratio = 65:35; d) conformer ratio = 8:2; e) conformer ratio = 9:1; f) conformer ratio = 75:25.

Received: November 25, 2014
Revised: December 12, 2014
Published online on ■■ ▮▮, 0000

Less talk, more actin: X-ray-structure-based in silico studies of the noncovalent interactions between complex polyketides and their natural target actin resulted in the design, modular synthesis, and biological evaluation of a novel and structurally simplified analogue class based on a hybrid structure of bistramide A and rhizopodin.

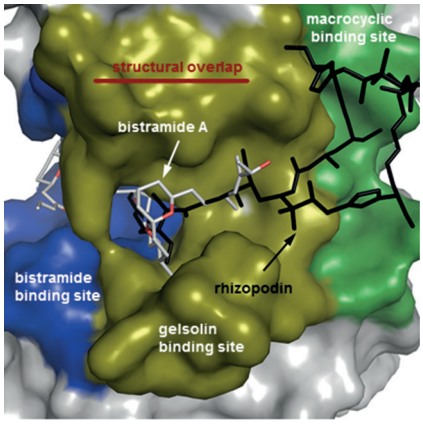

*D. Herkommer, S. Dreisigacker, G. Sergeev, F. Sasse, H. Gohlke, D. Menche**

■■ – ■■

Design, Synthesis, and Biological Evaluation of Simplified Side Chain Hybrids of the Potent Actin Binding Polyketides Rhizopodin and Bistramide

These are not the final page numbers! ↗↗